POROSITY REDUCTION IN A CAMBRIAN QUARTZ ARENITE GALESVILLE SANDSTONE, SOUTH CENTRAL WISCONSIN

Thesis for the Degree of M. S.

MICHIGAN STATE UNIVERSITY

THOMAS VINCENT WILSON

1977

ABSTRACT

POROSITY REDUCTION IN A CAMBRIAN QUARTZ ARENITE
GALESVILLE SANDSTONE, SOUTH CENTRAL WISCONSIN

By

Thomas Vincent Wilson

The Cambrian Galesville Sandstone of South Central Wisconsin was studied to determine the degree and mechanism of porosity reduction. The Galesville is a clean, well-rounded, well-sorted quartz sandstone which has never received more than 3,000 feet of sedimentary overburden.

Forty-four oriented samples of Cambrian Galesville Sandstone were obtained from stratigraphic grid samplings of bedding units at three sites near Baraboo, Wisconsin. Thin sections of the samples were analyzed for porosity using an antilog computer analyzer. Minus cement porosity and percent presolved quartz were determined from point counts of cathodo-luminescence photomicrographs. Thin section porosity measurements were confirmed by gas-expansion, mercury-emersion analyses.

Porosity of the samples in thin section range form 15.2% to 28.1%, averaging 19.7% (s=3.81, n=24), 20.8% (s=1.98, n=39), and 23.6% (s=1.35, n=24) for the three outcrop locations. Minus cement porosity averages 24.2% (s=3.60, n=47), 24.7% (s=2.58, n=72), and 23.6% (s=1.35,

n=24). Differences in porosity according to orientation are not statistically significant and the percentage presolved quartz is similar for all outcrops, averaging 0.80% (s=0.29, n=165).

Reduction in porosity due to mechanical re-packing of grains after deposition may have reduced porosity from approximately 49% to a minimum of 33%. Approximately 0.8% intergranular pressure solution in the Galesville has resulted in more than a 9% porosity reduction below values established for maximum mechanical compaction of randomly packed sands (Gaither, 1953, Scott, 1960; Rutgers, 1962). This small percentage of intergranular pressure solution, virtually undetectable under a normal petrographic microscope, is an extremely important factor in the porosity reduction of the Galesville Sandstone.

Further porosity reduction due to later cementation by authigenic quartz, adularia, kaolinite, and hematite is variable between outcrops. The volume of quartz cement is independent of the volume of intergranular presolved quartz.

POROSITY REDUCTION IN A CAMBRIAN QUARTZ ARENITE GALESVILLE SANDSTONE, SOUTH CENTRAL WISCONSIN

By

Thomas Vincent Wilson

A THESIS

Submitted to
Michigan State University
in partial fulfillment of the requirements
for the degree of

MASTER OF SCIENCE

Department of Geology

1977

ACKNOWLEDGMENTS

This work was made possible by the aid of Michigan State University who provided the most generous use of equipment and facilities. Financial assistance for which I am most grateful was provided by the Michigan State Department of Geology Award for Outstanding Research Proposal--Grant-in-Aid of Research, 1976.

Additional financial assistance was provided by grants from Sigma XI--Scientific Research Society of North America and The American Association of Petroleum Geologists. I am very thankful for their generosity and I hope to have justified their good faith.

I am highly indebted to Mr. Curt Conley of the Kansas Geological Survey for the personal consideration and assistance I received while in Lawrence, Kansas, and for the use of the Survey's computer image analyser.

I wish to thank the members of my thesis committee for their valuable assistance in the preparation and writing of this thesis. Dr. Duncan Sibley, serving as committee chairman, provided continued encouragement and interest in the progress of the research and testing of ideas. Dr. William Cambray, Dr. Thomas Vogel, and Dr. Harold Stonehouse were of great help in providing assis-

assistances and materials useful to the completion of research and in the preparation of the final written draft.

In addition, I would like to thank the members of the sedimentology seminar. Under the direction of Dr. Sibley, this group provided the opportunity to present current results and ideas as thesis research progressed. The suggestions and constructive criticisms generated helped provide a clear perspective on problems encountered and the proper direction of the research.

I wish to thank Mike Ritter for his continued technical assistance and advice. His maintenance of thin sectioning, laboratory and cathodo-luminescence equipment was invaluable to the completion of the research.

Special thanks go to Deb Kirchen for her work typing the final draft and for putting everything in order when I couldn't be there to help.

Finally, I wish to thank my wife, Linda, for her assistance in sample collection, preparation and for her encouragement and help during the long hours spent on the many phases of analysis. Most of all, I want to thank her for bearing up so well under a year of odd hours and inconvenience.

Thomas V. Wilson

August, 1977

TABLE OF CONTENTS

	Page
INTRODUCTION	1
GEOLOGIC SETTING - DEPOSITIONAL ENVIRONMENT	2
DEPTH OF BURIAL	6
SAMPLE COLLECTION	11
SAMPLE PREPARATION	11
LABORATORY ANALYSIS	13
Image Analysis	13
Cathodo-Luminescent Microscopy	18
DATA: IMAGE AND LUMINESCENT MICROSCOPE ANALYSIS	25
ACCURACY OF IMAGE ANALYSIS POROSITY DETERMINATIONS	28
POROSITY VARIATIONS	32
MECHANICAL POROSITY REDUCTION	38
PRESSURE SOLUTION	42
MODELING POROSITY REDUCTION DUE TO PRESSURE SOLUTION	43
RELATIONSHIP BETWEEN MECHANICAL POROSITY REDUCTION AND REDUCTION BY PRESSURE SOLUTION	45
LARGE SCALE EFFECTS OF POROSITY REDUCTION	50
CONCLUSIONS	51
RECOMMENDATIONS FOR FURTHER STUDY	53
BIBLIOGRAPHY	54

APPENDIDICES

Appendix Page

A. Description of Sampling Locations 57

B. Porosity Reduction due to Pressure Solution in Hexagonally Close-Packed Spheres. 60

C. Data: Image Analysis and Point Counts of Cathodo-Luminescence Microscope Photographs . 65

LIST OF TABLES

Table		Page
1.	Estimated Thickness of Strata Above the Galesville Sandstone, Baraboo, Wisconsin	9
2.	Image Analysis: Second Operator Comparison. . .	16
3.	Comparison with Unknown Analyses	17
4.	Multiple Analyses of Thin Sections	19
5.	Data: Image and Luminescent Microscope Analyses	27
6.	Point Count Porosity - Incompletely Impregnated Samples, Outcrop One	30
7.	Mean Thin Section Porosity Determined by Point Counts, Outcrop One.	31
8.	Core Laboratory Versus Thin Section Porosity Analyses.	33
9.	Image Analysis Porosity: Directional Comparison of N-S and E-W Vertical Thin Sections	36
10.	Image Analysis Porosity: Directional Comparison of Horizontal and Vertical Thin Sections	37
11.	Image Analysis of Disaggregated Galesville Sandstone Thin Sections.	40
12.	Porosity of Disaggregated Galesville Sands Determined by Volume-Density Analysis.	41
13.	Compaction of a Hexagonally Close-Packed Arrangement of Spheres	63

LIST OF FIGURES

Figure			Page
1.	a.	Galesville Grain Size Distributions from Thin Sections	3
	b.	Grain Size Distributions of Other Mature Quartz Arenites	4
2.		Major Structural Features Surrounding the Baraboo Syncline Area	5
3.		Outcrop Locations and Units Sampled	12
4.		Blue Grain Size Distribution Compared with Distribution of Total Grain Population.	23
5.		Estimating Presolved Areas Between Spherical and Oblong Rounded Grains	26
6.		Porosity Reduction Due to Pressure Solution for Five Packing Arrangements of Spheres.	44
7.		Unit Cell of a Hexagonal Lattice.	46
8.		Pressure Solution to Porosity Reduction Relationships	48
9.		Pressure Solution Relationships During Vertical Compaction of the Hexagonal Model	61
10.		Percent Pressure Solution Versus Percent Porosity Reduction for Hexagonally Close-Packed Spheres	64

INTRODUCTION

The purpose of this study is to determine the quantitative contribution of each important diagenetic process to the resultant porosity reduction in a quartz arenite. The porosities of recent, unlithified sands have been well established (Pryor, 1973), as have the porosities in a great many ancient sandstones. However, the quantitative effect of processes reducing porosity during diagenesis have not, as yet, been well defined. This gap in knowledge is due largely to the lack of detailed petrographic analyses of sandstones, and the complication of uncontrolled variables in texturally and compositionally complex sandstones. To eliminate complex variables which affect porosity reduction, this study has been restricted to a single quartz arenite, the Galesville Sandstone (Cambrian) of South Central Wisconsin.

The porosity in the Galesville Sandstone and other ancient quartz arenites is lost by mechanical grain adjustments, intergranular pressure solution, and cementation. By thin section and volumetric porosity determinations, cathodoluminescence analysis; determining the porosity of disaggregated and artificially packed Galesville sands, the important variables in porosity loss have been defined and the mode of porosity reduction in the Galesville Sandstone has been determined.

GEOLOGIC SETTING - DEPOSITIONAL ENVIRONMENT

The Upper Cambrian Galesville Sandstone in South Central Wisconsin is a "blanket" sandstone deposit, approximately 100 feet thick consisting of white, friable, well-rounded, well-sorted, medium-grained pure quartz sand (Thwaites, 1930; Wanenmacker et al 1934; Raasch, 1935; Twenhofel, 1935; Driscoll, 1959; Emrich, 1966; Ostrom, 1966; Dalziel, Dott, and Black, 1970). The size distribution of the Galesville Sandstone is illustrated in Figure 1a. The long axes of 300 grains were measured for each of the six bedding units sampled and the results were compared with results of Friedman, 1961 (Figure 1b), who graphed the grain size distribution for other quartz arenites determined by sieve and thin section measurements.

The Galesville crops out on the Wisconsin Arch--South Wisconsin Highland (Figure 2). In the vicinity of Baraboo Wisconsin, the Galesville was deposited around erosional remnants of the Precambrian Baraboo Quartzite.

The Galesville was deposited in an aeolian--shallow marine environment. Evidence has been cited for the existence of both aeolian and shallow marine environments in and around the Baraboo syncline. It has been suggested (Dalziel, Dott, and Black, 1970; p. 52) that the local strand lay slightly offshore from the quartzite cliffs. This interpretation would put aeolian sands against and amongst the Baraboo cliffs, with shallow marine sands

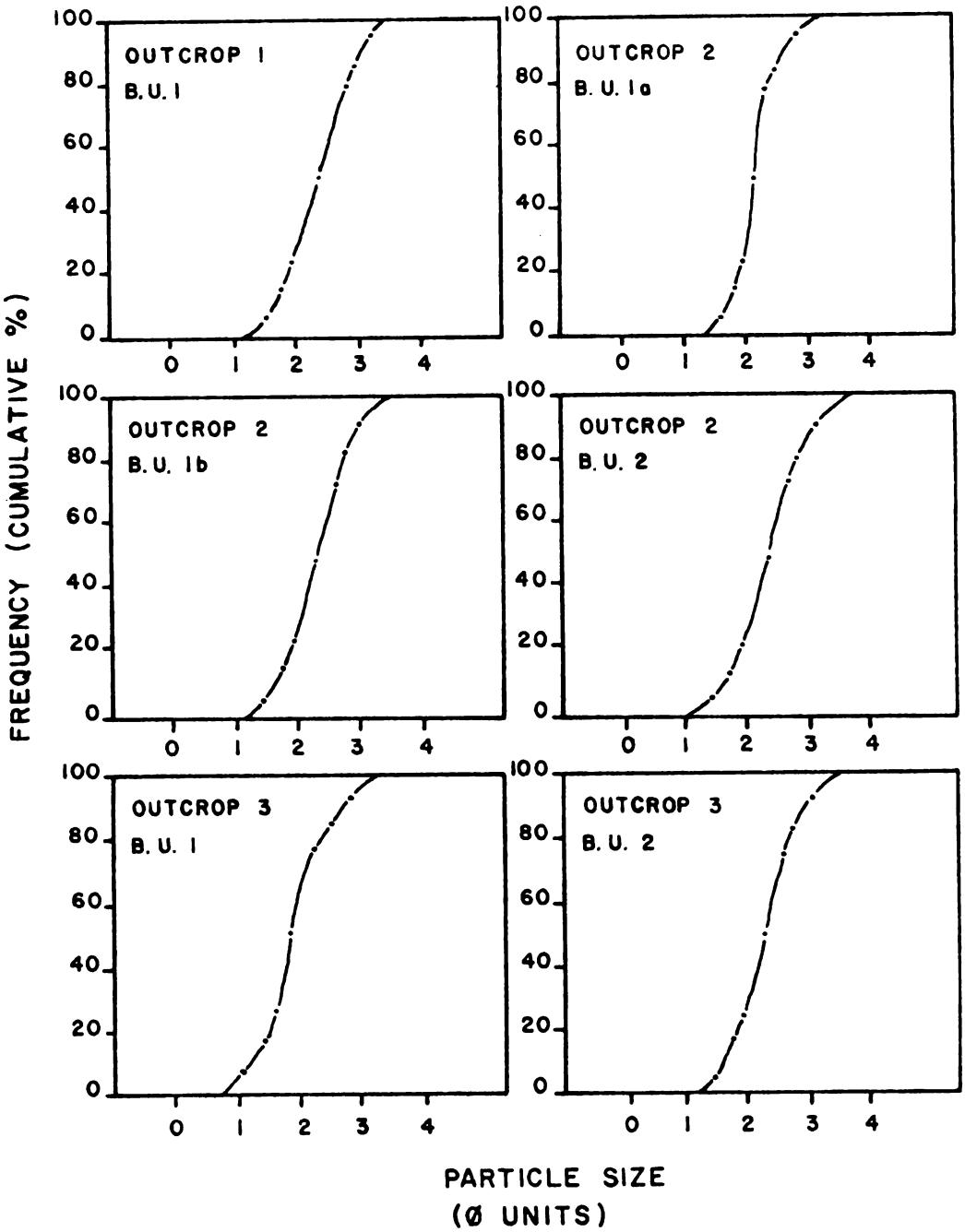

Figure 1a--Galesville Grain Size Distributions From Thin Sections

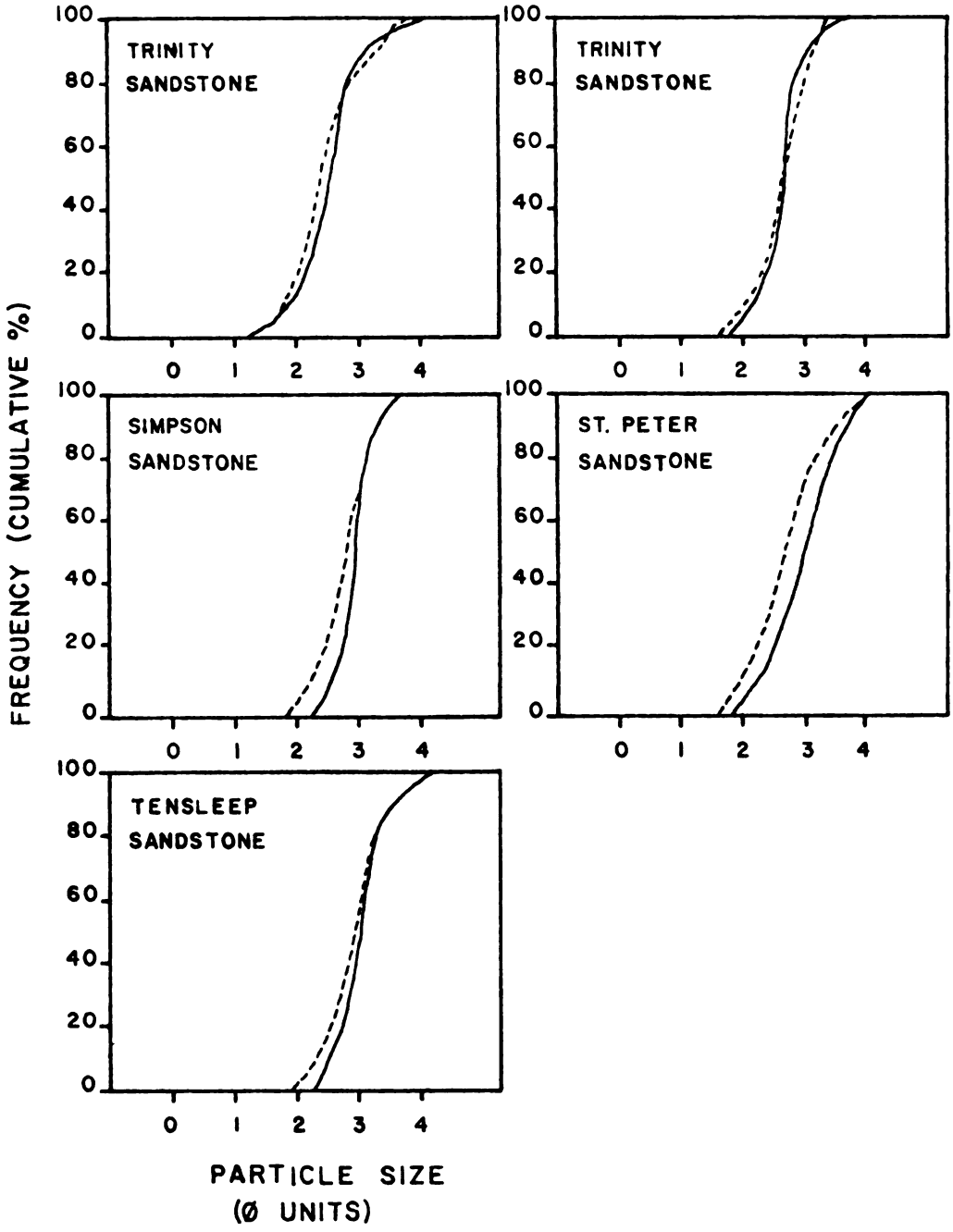

Figure 1b—Grain Size Distributions of Other Mature Quartz Arenites (After Friedman, 1961)

Figure 2 --Major Structural Features Surrounding the Baraboo Syncline Area. (After U.S.G.S. National Atlas 1970)

surrounding the syncline. Evidence supporting the interpretation is the occurrence of angular blocks of the Baraboo Quartzite in the Galesville adjacent to the cliffs and also the bi-modal size distribution of the sands adjacent to the Baraboo Cliffs.

The evidence, however, is often conflicting depending on location or stratigraphic position within the Galesville. Bi-modal distributions are not restricted to the cliffs; surf-rounded Baraboo clasts are found against the cliffs in several locations and large pebbles have been carried several miles south of the syncline by marine currents. Large scale cross-bedding indicative of near shore marine sands (Hamblin, 1961) is found in and around the syncline in various locations.

DEPTH OF BURIAL

In order to relate porosity reduction to the depth of burial of the Galesville Sandstone, it is necessary to determine the thickness of overlying stratigraphic units during the time of maximum burial. The Baraboo area, which is centered upon the Wisconsin Arch--South Wisconsin Highland, has been a structural high since late Cambrian time. Evidence for the structural high is provided by rapid thinning of sedimentary deposits to the east, south, and west toward the arch. Thinning is due to both a reduced volume of sediments deposited and numerous erosional disconformities. Sedimentation on the arch is characterized

by deposition of thin sedimentary units alternating with erosional intervals of various duration. Erosional effects become more prominant further onto the arch and northward (Cohee, 1948; Willman, et al 1975).

From strata represented in the Michigan and Illinois Basins, it can be inferred that the Wisconsin Arch at one time may have been covered by strata from Cambrian to Devonian in age (Schuchert, 1955) and possibly by strata as young as Pennsylvanian. It is debatable whether Cretaceous and/or Tertiary units were deposited in the area of the Wisconsin Arch. However, the compactive effect on the underlying strata due to their deposition would have been minimal because; 1). great thicknesses of sediments would not have been deposited in this stable interior, arch-highland area. 2). preceeding Triassic and Jurassic erosion would already have removed a substantial portion of the sedimentary column.

The total depth of burial of the Galesville Sandstone in the Baraboo area cannot be precisely determined due to the erosion of units of Chazyan Age and younger. For the most part, however, the record of deposition is intact in the Michigan and Illinois Basins. An estimate of the maximum thickness on the arch can be provided by establishing the thickness of each complete stratigraphic unit to the east, south, and west, nearest to Baraboo, Wisconsin. The estimate of stratigraphic thickness calculated will be

a maximum because of the overall thickening of the measured sedimentary column into the adjacent areas (see Table 1.)

Glaciation and loading by Pleistocene ice accumulation was not an important factor in compaction of the Paleozoic sediments. The Paleozoic sedimentary column overlying the Galesville in the Baraboo syncline area had been for the most part, eroded off pre-Pleistocene and was not a factor in loading and compaction during later glacial episodes. Samples were collected from what is known as the "driftless area" of Wisconsin. Although some evidence of glaciation is present in the sampled area near Baraboo (Dalziel, Dott, and Black 1970, p.71), ice thickness presumably was not excessive. For the overburden pressure on the Galesville Sandstone to exceed that due to the previous sedimentary overburden, an ice thickness of over 6,500 feet is required. The occurrence of an ice mass approaching this thickness in the driftless area of Wisconsin is highly unlikely.

Considering the maximum stratigraphic thicknesses into the structural basins adjacent to the Baraboo area, the maximum burial of the Galesville Sandstone is estimated to be 3,000 feet. The maximum lithostatic pressure resulting from 3,000 feet of overburden is estimated as approximately 200 atmospheres, considering the density of the sedimentary column to be 2.3 g/ccm. The actual lithostatic pressure affecting the Galesville was less, due to the hydrostatic pressure of the pore fluid.

Table 1: Estimated Thickness of Strata Above the Galesville Sandstone Baraboo, Wisconsin

Michigan Basin

Age	Location	Maximum Thickness (ft.)	Reference
Cambrain-M. Ordo.	S. Central Wisc.	455'	Ostrom (1967)
Upper Ordo.	S.W. Mich.	200'	Cohee (1948)
Silurian	S.W. Mich.	500'	Melhorn (1958)
Devonian	S.W. Mich.	200'	Fisher* (1977)
Early Miss.	W. Mich.	550'	Chung (1973)
Late Miss.		(?)	
Penn.		(?)	
		1,905'	

*Personal Communication

Illinois Basin

Age	Location	Maximum Thickness (ft.)	Reference
Cambrain	S. Central Wisc.	235'	Ostrom (1967)
Ordo.	N.E. Ill.	900'	Willman et at (1975)
Silurian	N.E. Ill.	300'	Willman et at (1975)
Devonian	Central Ill.	200'	Willman et at (1975)
Miss.		eroded	Willman et at (1975)
Penn.	N. Central Ill.	200'	Willman et at (1975)
		1,835'	

Table 1: Continued

Upper Mississippi Valley

Age	Location	Maximum Thickness (ft.)	Reference
Cambrain-M. Ordo.	S. Central Wisc.	455'	Ostrom (1967)
Upper Ordo.	Up. Miss. Valley	245'	(2)
Silurian	Up. Miss. Valley	375'	(2)
Devonian	Up. Miss. Valley	665'	(2)
Miss.	Up. Miss. Valley	856'	(2)
Penn.	Up. Miss. Valley	(?)	(2)
		2,596'	

(1) Sections measured may be up to 400 miles west and southwest of Baraboo. Thicknesses of units are substantially reduced toward arch.

(2) Kansas Geological Society Guidebook (1935).

SAMPLE COLLECTION

Samples were collected from three outcrop locations relative to the Baraboo syncline: 1). on the margin; 2). inside; 3). outside (Figure 3). Locations relative to the Baraboo quarzite cliffs forming the Baraboo syncline were chosen to represent the greatest possible variation in the compositional and textural characteristics of the sands due to different environments of depositions. Sampling was also designed to determine if porosity variations were present within individual bedding units and between bedding units at outcrop locations.

At each outcrop, separate bedding units were sampled by imposing a grid upon each unit. Grids varied in size depending on bedding unit character, ranging from three to nine feet in length. Each grid contained thirty sample intersections. Sample grids were adjusted to an angle of between twenty and thirty-five degrees relative to bedding to insure a proper stratigraphic sampling (Griffiths, 1967, p. 18; Chayes, 1956, Figure 8, p. 26). Samples taken at each grid point intersection were marked for north and horizontal orientation.

SAMPLE PREPARATION

Forty - four samples were randomly selected from over one hundred fifty grid point locations at the three Galesville outcrops. Samples were impregnated with red-dyed,

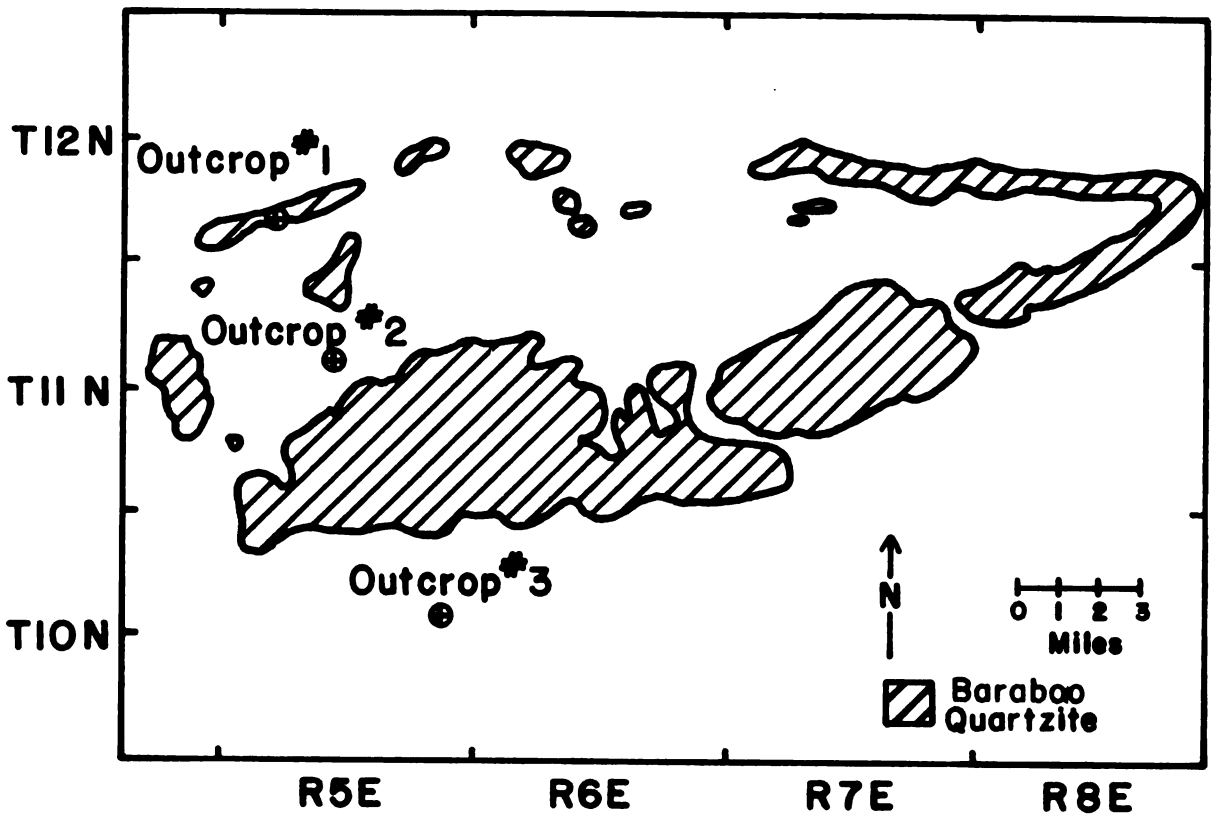

Outcrop One
- Bedding Unit 1

Outcrop Two
- Bedding Unit 1a
- Bedding Unit 1b
- Bedding Unit 2

Outcrop Three
- Bedding Unit 1
- Bedding Unit 2

Figure 3--Outcrop Locations and Units Sampled
(Map after Wanenmacher, J.M. 1935)

low viscosity epoxy resin (Minoura and Conley, 1971) and sectioned in north-south and east-west vertical orientations. Eighteen selected samples were also sectioned horizontally. Sections were ground to thirty microns thickness and then polished for cathodo-luminescent petrography.

Galesville sands from two of the grid samplings were disaggregated and packed in twelve separate containers. Four sands were tightly packed by shaking and tamping, four sands were loosely packed by shaking, and four were left unpacked after pouring. These disaggregated sands were then impregnated with red epoxy and thin sectioned.

LABORATORY ANALYSIS

Image Analysis

Thin sections of impregnated Galesville Sandstone samples and of disaggregated and impregnated Galesville sands were taken to the Kansas Geological Survey office in Lawrence, Kansas, for porosity analyses on the Survey's computer image analyzer. The image analysis equipment consists of six main components:

1). Petrographic Microscope: Microscope is provided special lighting, light filtering, and lenses to provide an even distribution of light intensity within the field of view.

2). Black and White Television Camera: Mounted on the microscope, the vidicon camera provides good

resolution between areas of different light intensity on the thin section.

3). Color Monitor Display: Color television displays the field analyzed for percent porosity.

4). VP 8 Processor Control Console: Controls color intensity and provides direct digital read-out of percent pore space.

5). MAF 1, Moving Area Framer: Defines the dimensions of the area or "window" on the monitor within which porosity will be calculated.

6). Hewlett-Packard 1310 A, X-Y-Z Display Cathode Ray Tube: Displays voltage levels within field of view so adjustment can be made for maximum differentiation between areas of differing light intensity.

The system operates by continually scanning (30 times/second) the thin section image within the area specified by the window adjustment. Along each line of scan, signals of high and low voltage are produced on areas of light and dark coloration. Because of the intense color of the red epoxy, pore spaces are seen as much darker than the transparent quartz grains.

Adjustment is made with the aid of the cathode ray tube so that a significant voltage difference exists between light and dark areas within the field. A threshold level is then selected by the operator to best delineate high and low voltage areas. The selection is made by adjusting the boundary between quartz grains and red epoxy as it appears

on the color monitor. The computer then totals the length of the scan below the theshold level and displays it digitally as percent porosity.

The mean porosity of each thin section was determined by measuring and averaging the porosity within 36-1.5 mm square areas randomly chosen on the slides. Possible sources of error for porosity measurements lie in poor focusing of the petrographic scope and misadjustment of the grain-epoxy boundary. Despite the precision indicated by the low standard deviation values, four separate tests were conducted to determine the significance of any possible error:

1). Second operator comparison: Mr. C.D. Conley of the Kansas Geological Survey ran second analyses on fourteen thin sections representing the three outcrop locations. Conley's result differed from the first set of analyses by an average of only 0.4% per thin section. The means for the two sets of analyses by t-test were not statistically different (Table 2).

2). Unknown analysis: Twenty-four samples were analyzed for percent porosity without previous knowledge of the samples' origin. Results for the unknowns were also not statistically different and varied from initial results by an average of 0.15% per thin section (Table 3).

3). Multiple analyses: Three slides were chosen for multiple analyses to establish the variation which may be expected in the repeated analysis of one slide. Six analyses were performed on each of the three slides. A maximum

Table 2: Image Analysis, Second Operator Comparison

Sample #	% Porosity C.D. Conley S		% Porosity T. Wilson S		Difference
1-10E	12.6	3.1	14.0	3.5	-1.4
2-4N	22.6	2.4	24.1	2.4	-1.5
3-28E	19.4	2.1	17.8	2.3	+1.6
4-9N	24.4	3.2	23.3	2.5	+1.1
4-9N	20.2	2.8	23.3	2.5	-3.1
4-9N	20.3	3.5	23.3	2.5	-3.0
5-8E	19.7	2.0	20.6	2.2	-0.9
5-8E	19.3	1.9	20.6	2.2	-1.3
5-8E	18.1	2.1	20.6	2.2	-2.5
6-6N	22.0	2.5	20.1	2.3	+1.9
6-6N	19.6	2.1	20.1	2.3	-0.5
6-6N	21.3	2.6	20.1	2.3	+1.2
5-5L-C-2	36.6	3.5	35.8	2.6	+0.8
5-5L--C-2	37.3	2.7	35.8	2.6	+1.5

Mean Difference Per
Thin Section = 0.44%

Table 3: Comparison with Unknown Analyses

Sample #	% Porosity Unknown Analysis	$\bar{S}$	% Porosity Initial Analysis	$\bar{S}$	Difference
1-10E	14.0	2.24*	14.0	3.53*	0.0
1-18N	16.6	3.08	10.2	2.26	+6.4
1-22N	13.1	1.98	12.5	2.21	+0.6
2-3E	26.3	2.57	23.6	3.34	+2.7
2-4N	24.5	2.09	24.1	2.42	+0.4
2-5N	24.3	2.44	24.1	2.61	+0.2
3-6E	21.9	1.98	19.1	2.51	+2.8
3-18E	19.8	2.41	19.3	3.68	+0.5
3-25E	17.6	2.31	19.0	2.91	-1.4
2-4Ea	25.8	3.85	23.3	3.11	+1.5
4-9N	23.8	2.69	23.3	2.54	+0.5
4-12N	22.5	2.55	23.2	2.24	-0.7
5-11N	18.1	1.95	22.9	2.00	-4.8
5-12N	21.1	2.14	23.2	2.77	-2.1
5-13Eb	18.0	1.71	20.1	1.70	-2.1
6-23N	24.3	3.06	22.9	3.06	+1.4
6-25N	24.5	2.54	25.1	1.84	-0.6
6-29N	21.7	3.62	23.8	2.73	-2.1
3-29L-A-2	44.8	3.72	45.1	2.18	-0.3
3-29L-B-1	36.5	1.86	35.9	2.24	+0.6
3-29L-C-1	36.5	1.97	34.3	2.49	+2.2
3-29L-A-1	41.6	2.14	42.2	1.98	-0.6
3-29L-B-2	37.3	2.63	36.3	2.54	+1.0
3-29L-C-2	34.0	2.40	33.7	2.38	+0.3

Average Error/Analysis = 0.27%

*n=36 for all analyses

range between high and low determinations of 1.9% porosity was obtained for measurements within the three groups. Standard deviations for the three groups were all less than 0.70 for six determinations (Table 4).

4). Image analysis versus point counts: Fields which had porosities computer analyzed were photographed from the monitor. Point counts were made by Mr. C.D. Conley on photographic enlargements of the fields. Mean results for image analysis and point count porosities were well within statistical error on a 95% confidence level by t-test of mean values.

Cathodo-Luminescent Microscopy

In thin sections of clastic sedimentary rocks, the cathodo-luminescent microscope can serve to distinguish detrital grains from authigenic overgrowths by their different luminescing qualities (Sippel, 1968).

The vast differences between the conditions of crystallization in originally high temperature detrital grains and low temperature authigenic overgrowths result in lower concentrations of trace impurities within the crystal lattices of the authigenically precipitated mineral or minerals. Electron bombardment of minerals in a helium-filled chamber causes trace impurites in the original detrital grains to undergo electron excitment and subsequent emission of visible light spectra. Differing coloration or intensity of the emission can distinguish detrital grains from overgrowths.

Table 4: Multiple Analyses of Thin Sections

Sample #	% Porosity	Std. Dev.	n
5-5L-A-1	43.6	3.19	36
	43.3	3.14	36
	44.6	2.72	36
	44.2	2.81	36
	42.7	3.21	36
	43.4	2.00	36
Mean Porosity =	43.6	0.68	6
5-5L-B-1	38.2	2.96	36
	38.7	2.43	36
	38.8	2.59	36
	38.0	2.58	36
	37.8	2.68	36
	38.0	2.57	36
Mean Porosity =	38.3	0.37	6
5-5L-C-2	35.7	2.32	36
	36.5	2.55	36
	35.2	2.89	36
	35.4	2.15	36
	34.7	2.33	36
	36.2	2.34	36
Mean Porosity =	35.6	0.66	6

This is especially useful in the case of quartz where overgrowths are optically continuous with detrital quartz grains under plane and polarized light.

In order to determine the necessity for cathodo-luminescence analysis, Galesville thin sections were first examined to determine if the volume of quartz cement could be estimated under a normal petrographic microscope using "dust ring" evidence alone. For slide containing the best developed dust rings in the Galesville, approximately one third of the points near grain margins could not be definitely classed as grain or overgrowth. It is concluded that dust rings are too discontinuous to provide a basis for accurate quantitative estimates of the volume of authigenic quartz. In addition, because of the discontinuous nature of the dust rings, an accurate estimate of the degree of intergranular pressure solution using dust rings is not possible. Using sutured grain contacts as an indicator of pressure solution was also excluded because of their extremely limited occurrence.

Approximately six hundred color photographs were taken of Galesville thin sections. Two photographs were taken for each 2.2 x 1.4 mm fields to be analyzed, one under transmitted plane light and the second under cathodo-luminescence. When compared, the two photos define the position of detrital grain-overgrowth boundaries.

Two fields, randomly chosen, were photographed for each of eighty-two thin sections. In addition, six thin

sections representing the six bedding units (Figure 3) were photographed for twenty different fields per slide. Multiple analyses were performed in order that the variation observed within an outcrop could be compared with the variation present within a single thin section.

Luminoscope photographs were taken using fifteen minute exposures on high speed ektachrome light film (ASA 125) and specially processed, pushing the ASA to 325. The luminoscope was manufactured by Nuclide Corporation, model number ELM 23. Beam energy was set at 14KV from a cold cathode-ray tube. A beam current setting of 0.6 ma was used.

Color slides were projected into a light-table display, carefully adjusted to eliminate optical distortion. On the table, detrital grain and overgrowth margins were traced on graph paper. Areas within the grains and overgrowths were determined by summing the number of points of intersection on the graph paper within the respective areas. The volumes of detrital quartz and overgrowth are proportional to the areas measured by point counting. After grain to cement ratios were determined, the minus cement porosities of the thin sections were calculated by adding the proportional cement volume to the image analysis porosity.

A problem in the determination of detrital grain overgrowth boundaries was present in many Galesville thin sections due to a slight reddish luminescence of the overgrowths. Boundaries became difficult to locate when detrital grain centers luminesced similar shades. To avoid possible

difficulties with interpreting these slight variations, only grains luminescing bright blue were analyzed for grain to cement ratios. For each of the four outcrops where minus cement porosities were calculated, blue grain size distributions were checked, and proved nearly identical to the overall size distributions measured in thin section (see Figure 4). Differing size distributions would have resulted in a biased grain to cement ratio. No tendency toward overgrowths preferentially covering differently colored luminescing grains was observed.

Percent intergranular pressure solution was estimated on luminescence photographs by reconstructing rounded grain boundaries where penetration by adjacent grains had occurred and measuring the area of penetration by point counts on graph paper. The resulting estimate is somewhat subjective in that it requires the petrographer to reconstruct boundaries which have been destroyed by penetration of the two grains. However, in well-rounded sands this reconstruction is relatively straightforward.

At outcrops one and two where only blue luminescing grains were used, the percent pressure solution was calculated by proportionally correcting the presolved quartz: total quartz ratio determined by point counts to the total rock volume. At outcrop three where no quartz cement was present, an estimate of the presolved volume was obtained by measuring the presolved areas at penetrating grain contacts as observed in plane light.

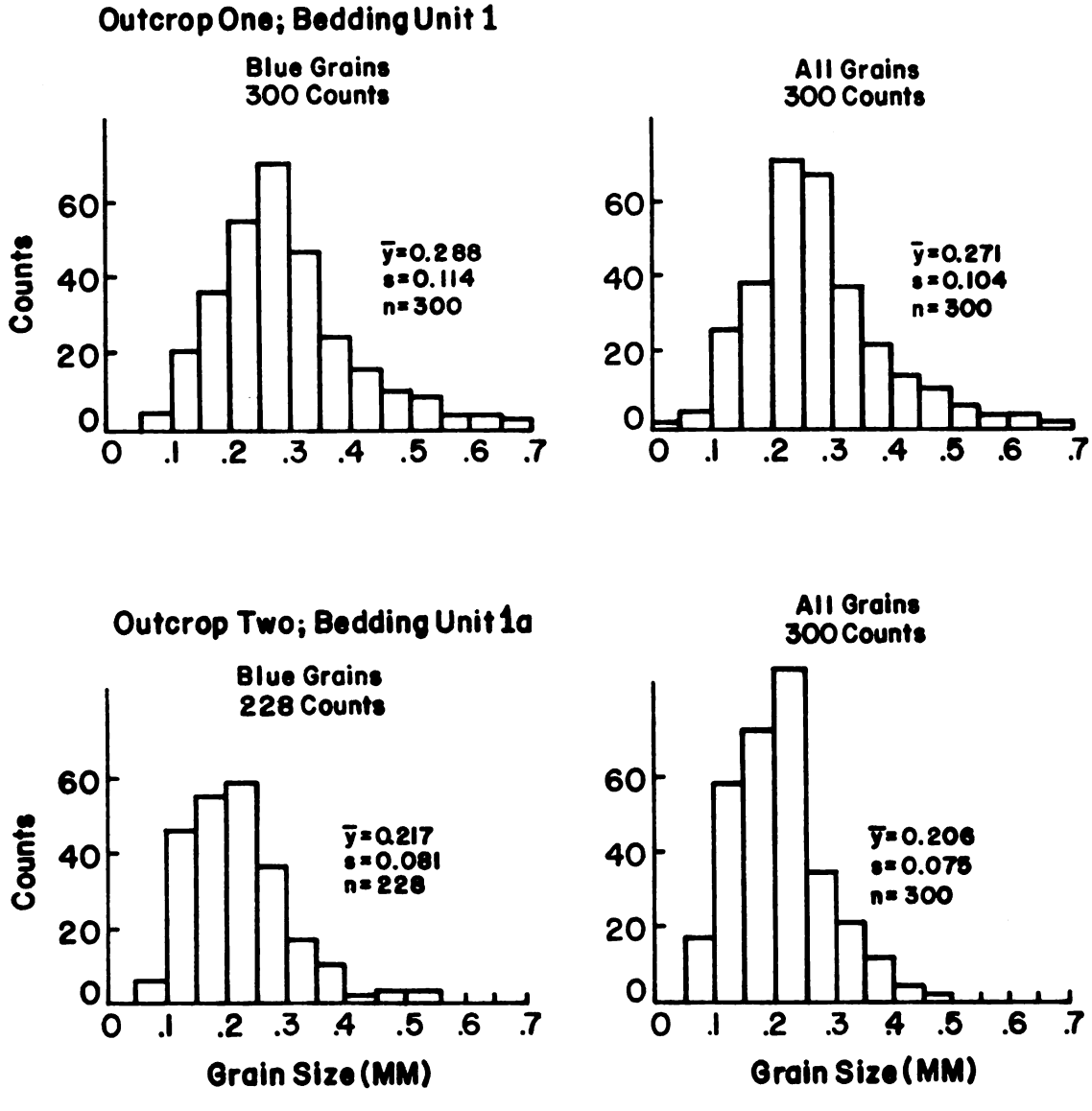

Figure 4--Blue Grain Size Distribution Compared with Distribution of Total Grain Populaiton

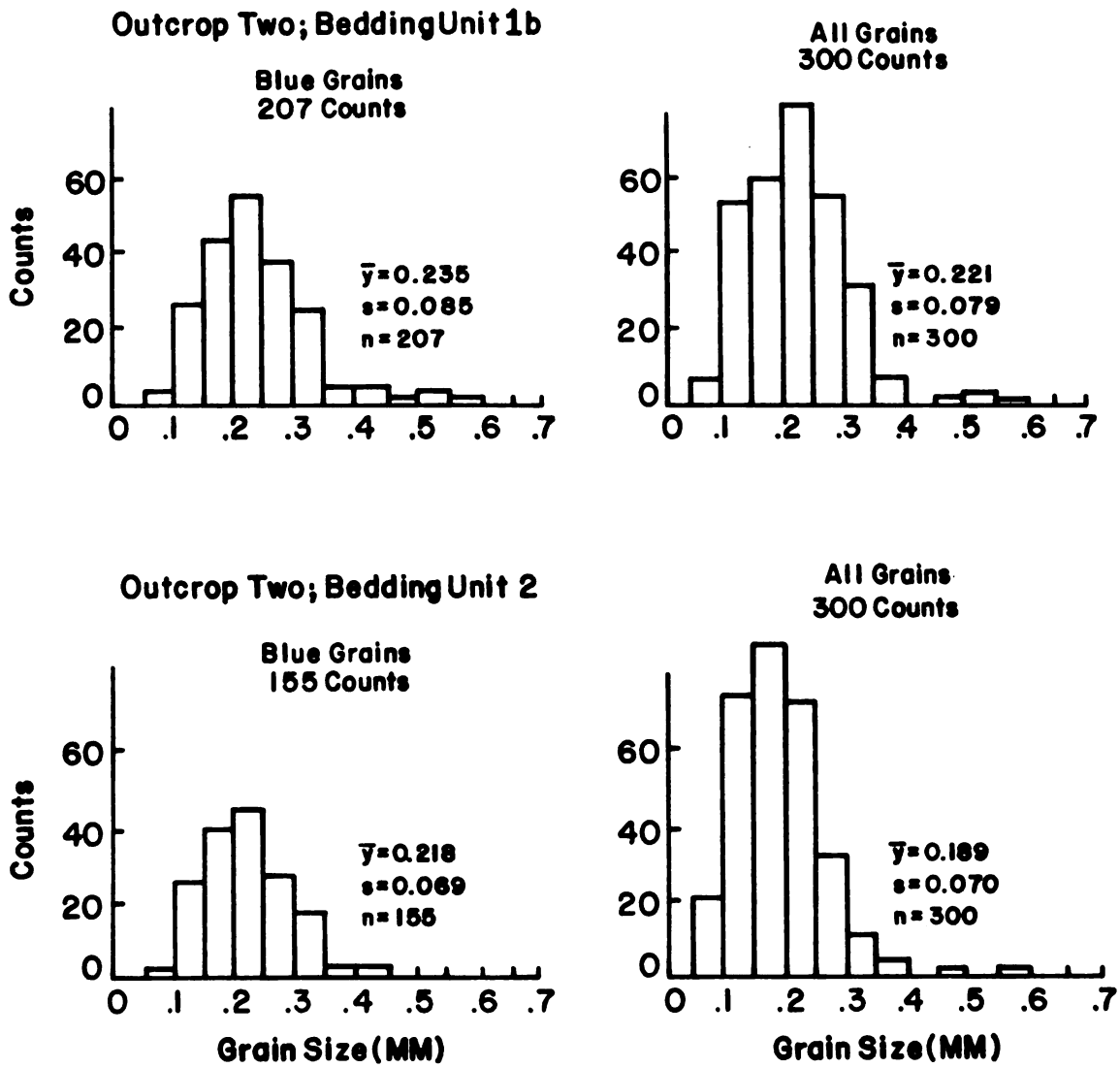

Figure 4--(cont'd)

Sketching presolved grain boundaries and determining the percentage of pressure solution by point counting should provide a maximum estimate of intergranular presolved quartz. Long grain contacts were considered presolved contacts, with the degree of penetration established by the shapes of the grains approaching the contact (Figure 5). Presolved grain areas were estimated liberally.

Authigenic adularia is present at outcrops two and three being easily identified by its characteristic dull green luminescence. The percentage of adularia was estimated from slides of outcrop two by point-counting fields containing adularia traced on graph paper. Only trace quantities of adularia were present at outcrop three, precipitated on a small fraction of silt-sized detrital feldspar grains. The exact percentage was not determined because of the relatively small volume, and because the extremely bright blue luminescing detrital feldspars made grain-overgrowth boundaries difficult to distinguish.

DATA: IMAGE AND LUMINESCENT MICROSCOPE ANALYSIS

Mean values of percent plus and minus cement porosity, percent presolved quartz, percent quartz cement and percent adularia from each bedding unit are listed in Table 5. Mean values for each outcrop are totaled below the bedding unit totals. The standard deviation of the mean, as well as the number of samples measured, are listed in parentheses.

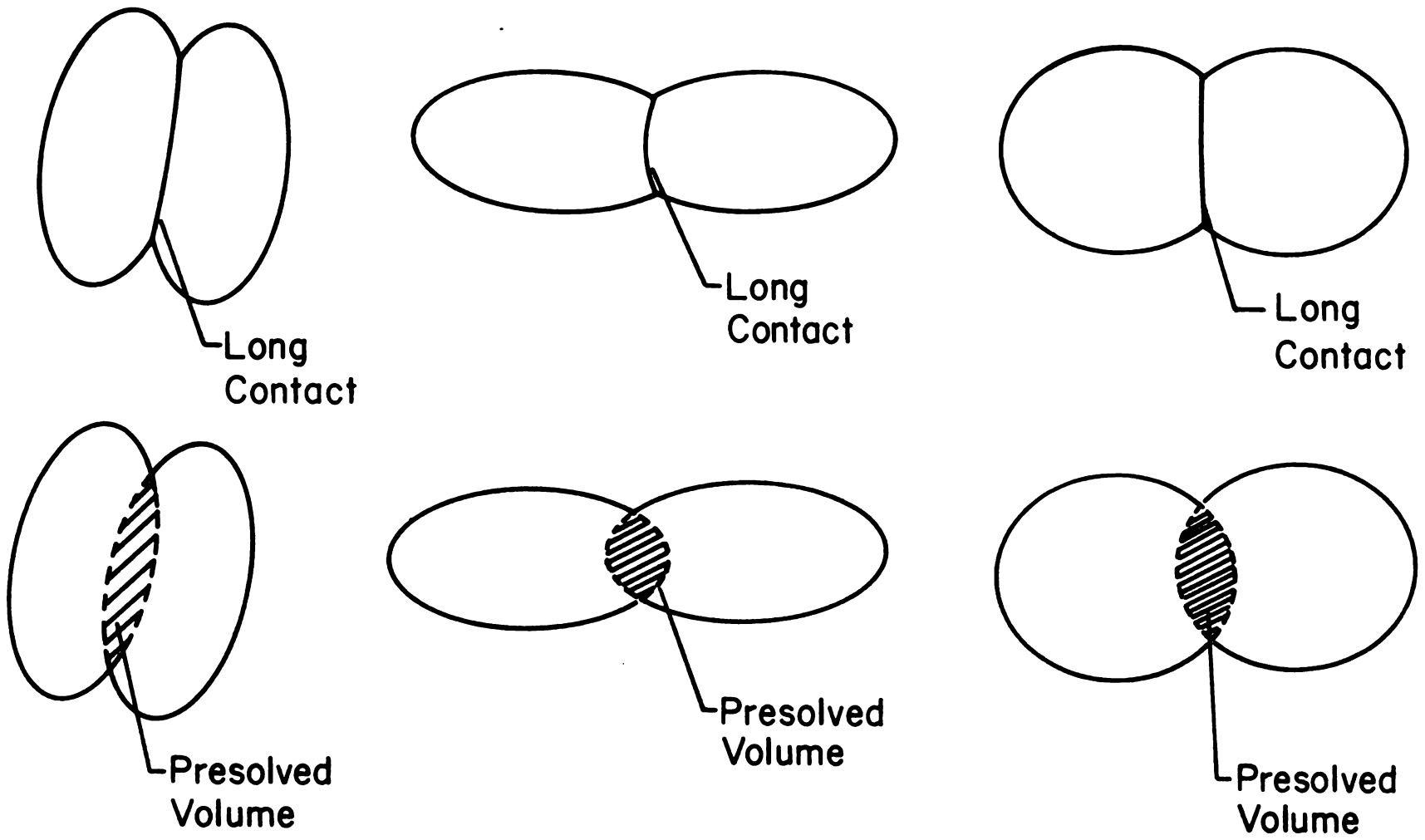

Figure 5--Estimating Presolved Areas Between Spherical and Oblong Rounded Grains

Table 5: Data: Image and Luminescent Microscope Analysis

% Porosity	% Pyrobitumen

Table 5: Data: Image and Luminescent Microscope Analysis

	% Porosity Image Anal.	% Presolved Qtz.	% Qtz. Cement	% Adularia	% Minus Cement Porosity
OUTCROP #1					
*Bedding Unit 1	12.8 % (s=2.05, n=24)	0.80 % (s=0.65, n=46)	4.9 % (s=2.77, n=46)	0.0 %	17.7 % (s=3.34, n=46)
OUTCROP #2					
Bedding Unit 1A	19.4 % (s=1.72, n=14)	0.91 % (s=0.63, n=22)	3.6 % (s=1.70, n=22)	0.25 % (s=0.31, n=22)	23.3 % (s=2.76, n=22)
Bedding Unit 1B	20.7 % (s=1.69, n=14)	0.82 % (s=0.53, n=28)	4.3 % (s=1.91, n=28)	0.53 % (s=0.72, n=28)	25.5 % (s=2.82, n=28)
Bedding Unit 2	22.7 % (s=1.51, n=11)	0.62 % (s=0.52, n=22)	1.7 % (s=1.31, n=22)	0.91 % (s=1.29, n=22)	25.3 % (s=1.70, n=22)
Totals	20.8 % (s=1.98, n=39)	0.79 % (s=0.56, n=72)	3.29 % (s=1.94, n=72)	0.56 % (s=0.71, n=72)	24.7 % (s=2.58, n=72)
OUTCROP # 3					
Bedding Unit 1	24.2 % (s=1.64, n=11)	0.90 % (s=0.36, n=22)	0.0 %	0.0 %	24.2 % (s=1.64, n=11)
Bedding Unit 2	23.1 % (s=0.70, n=13)	0.86 % (s=0.30, n=25)	0.0 %	0.0 %	23.1 % (s=0.70, n=13)
Totals	23.6 % (s=1.35, n=24)	0.88 % (s=0.34, n=47)	0.0 %	0.0 %	23.6 % (s=1.35, n=24)

* See Table 6 for point count results.

Individual thin section analyses upon which these mean values are based are listed in Appendix C.

ACCURACY OF IMAGE ANALYSIS POROSITY DETERMINATIONS

There is a problem in the accuracy of thin section analyses of porosity in sandstones which are mineralogically complex or contain quantities of clay. It is caused by the increasing volume of micropore space in sandstones with increasing mineral and textural complexity. In the analysis of clean, quartzose sandstones, however, the occurrence of micropore space is minimized. Rounded quartz grain boundaries are easily defined. Other mineral phases having porosity relationships difficult to distinguish in thin section are not present. In addition, impregnation of the Galesville Sandstone samples with low-viscosity, red epoxy resin also aides in distinguishing pores.

A variable quantity of clay and iron oxide is present at outcrop one. The clay was identified by x-ray analysis as kaolinite intermixed with iron hydroxides. Both the clay and the iron oxides are the result of leaching from the overlying soil horizon. In some thin sections, clay is seen to completely fill the pore spaces. Kaolinite is a late diagenetic phase and did not play a role in early porosity reduction due to compaction, pressure solution, or precipitation of quartz overgrowths. This is evidenced by the lack of clay along pressure

solution and cement intergrowth contacts. Because the precipitation of kaolinite clay occurred late in the diagenetic history of the Galesville, an estimate of its actual volume is not crucial to an understanding of porosity reduction. Clay merely fills pores which have already been defined by the earlier stages of diagenesis.

The presence of clay, however, complicates image analysis by impeding epoxy impregnation. Incomplete impregnation has resulted in excessive plucking in some slides during sample preparation. Porosities, as a result, are biased low. In order to estimate the effect of incomplete impregnation, point counts were made of all sections from outcrop one. Red epoxy, clay, and incompletely impregnated areas were counted as pore space (Table 6). The average porosity provided by these point counts provides a better estimate of this porosity between quartz grains and quartz overgrowths than the results of image analysis.

The mean point count porosity (Table 6) is used in place of image analysis porosity to calculate percent presolved quartz, percent quartz cement and percent minus cement porosity in Table 7. The point count porosity which eliminates the bias of impermeable clay results in a calculated minus cement porosity of 24.2%. This mean value is not statistically different from those measured by image analysis for outcrops two and three.

Table 6: Point Count Porosity - Incompletely Impregnated Samples; Outcrop One

Sample #	% Image Analysis Porosity	Point Counts: % Red Epoxy	Point Counts: Total % Porosity
1-EN	11.2	11.2	25.2
1-EE	13.8	23.2	29.8
1-FD	14.8	11.0	19.0
1-FS	16.1	16.7	21.3
1-6N	12.2	10.8	17.5
1-6E	11.4	12.7	15.7
1-7N	11.4	10.3	16.3
1-8N	13.7	10.5	15.2
1-8E	13.2	12.5	17.5
1-10Na	8.7	10.0	18.0
1-10Nb	14.6	15.0	16.0
1-10E	14.9	13.3	17.3
1-12N	14.0	17.0	18.3
1-12N	16.0	13.8	18.8
1-12E	15.8	15.2	21.8
1-13Na	12.0	10.2	17.5
1-13Nb	14.4	19.8	25.5
1-13E	11.8	9.5	16.3
1-18N	10.2	15.5	18.8
1-18E	10.0	10.8	25.8
1-19N	11.9	7.0	17.7
1-19E	10.5	13.5	18.2
1-22N	12.5	12.0	21.7
1-22E	11.2	18.7	23.3
Mean Porosity	12.8%	13.3%	19.7%
	(s=2.05)	(s=3.74)	(s=3.81)
	(n=24)	(n=24)	(n=24)

Table 7: Mean Thin Section Porosity Determined by Point Counts; Outcrop One

	% Porosity Point Counts	% Presolved Quartz	% Quartz Cement	% Minus Cement Porosity
Bedding Unit One	19.7	0.73	4.5	24.2
	s=3.81	s=0.57	s=2.37	s=3.60
	n=24	n=47	n=47	n=47

A final check of the accuracy of thin section porosity analysis was made by comparison with porosity measurements performed by Core Laboratories, Incorporated, on Galesville hand samples. Sample porosity was determined by helium expansion-mercury emersion (HE-ME). Results of Core Laboratory porosity measurements compared with image analysis determinations of the same samples are listed in Table 8. T-test of samples show no signif- - icant difference between mean values for the two methods of porosity measurement at outcrop two.

A small difference in mean values is discerned at outcrop three. The difference is due to the presence of silt-sized particles in several sections, not always visable within the red epoxy. This results in image analyses slightly higher than HE-ME determinations. A difference of 8.9% in the two mean porosities is present at outcrop one. As previously discussed, this is caused by the interstitial kaolinite at outcrop one, the volume of which was not determinable and thus eliminated from thin section analyses. While Core Lab porosity provides a better estimate of the actual sandstone porosity, point counts serve to determine the porosity before precipitation of kaolinite and iron cements.

POROSITY VARIATIONS

Comparisons were made of image analysis porosities according to the orientation of thin sections. Results

Table 8: Core Laboratory v.s. Thin Section Porosity Analyses

OUTCROP ONE

Sample #	% Core Lab Porosity	% Point Count Porosity	
		N-S	E-W
1-E	11.6	25.2	29.8
1-6	14.0	17.5	15.7
1-7	8.2	16.3	15.2
1-8	8.9	17.5	18.0
1-10	7.8	16.0 & 17.3	18.3
1-12	10.2	18.8	21.8
1-13	15.5 & 11.0	17.5 & 25.5	16.2
1-18	13.0	18.8	25.8
1-22	8.5	21.7	23.3
Avg. Porosity Outcrop One:	10.9% s=2.64 n=10	19.8% s=4.13 n=20	

OUTCROP TWO

Sample #	% Core Lab Porosity	% Image Analyses Porosity	
		N-S	E-W
3-16	17.4	17.7	20.6
3-30	19.8	18.2	17.9
5-12	22.6	23.2	21.4
5-15	22.6	21.5	22.5
6-6	20.8	20.1	20.2
6-25	20.8	25.1	24.0
Avg. Porosity Outcrop Two:	20.7% s=1.95 n=6	21.0% s=2.40 n=12	

Table 8: Continued

OUTCROP THREE

Sample #	% Core Lab Porosity	% Image Analyses Porosity	
		N-S	E-W
2-2	22.4	25.9	26.1
2-5	22.5	24.1	24.0
4-2	20.1	24.0	24.7 & 23.3
2-8	19.2	23.3	22.0
Avg. Porosity Outcrop Three:	21.1% s=1.66 n=4	24.2% s=1.29 n=9	

of the comparison for north-south versus east-west and horizontal versus vertical orientations are listed in Tables 9 and 10. The mean porosities compared by t-test show no statistical difference according to orientation in the Galesville.

Wide ranges in porosity of the Galesville are seen only on a very small scale. Variations in porosity between 1.5 mm areas on a thin section commonly range up to 12%; however, estimates of mean thin section porosity are very consistent between thin sections and bedding units for each outcrop location. Between outcrop locations plus cement porosity varies considerably due to varying quantities of authigenic quartz, adularia, kaolinite, and hematite.

Minus cement porosity measurements between the three Galesville outcrop locations do not differ significantly, only ranging from 23.6% to 24.7% (Table 5). In addition, individual thin sections are highly representative of the mean minus cement porosity present at all outcrops. Using data from Appendix C, the minus cement porosity for the four outcrops determined from eighty-four separate thin sections is not statistically different at the 95% confidence level from the average porosity determined from the multiple analyses of one section for each outcrop.

The percentages of intergranular presolved quartz were tested to see if significant differences existed between mean values for different sample groups.

Table 9: Image Analysis Porosity; Directional Comparison of N-S and E-W Vertical Thin Sections

		Avg.	Std. Dev.	n
Outcrop #1 - Bedding Unit 1				
	N-S Sections	12.9	1.75	12
	E-W Sections	12.1	2.18	10
Outcrop #2 - Bedding Unit 1a		Avg.	Std. Dev.	n
	N-S Sections	19.5	1.87	7
	E-W Sections	19.0	1.08	7
- Bedding Unit 1b				
	N-S Sections	20.7	1.71	7
	E-W Sections	20.6	1.50	8
- Bedding Unit 2				
	N-S Sections	23.0	1.57	6
	E-W Sections	22.3	1.53	7
Outcrop #3 - Bedding Unit 1		Avg.	Std. Dev.	n
	N-S Sections	24.9	1.59	6
	E-W Sections	24.3	2.05	7
- Bedding Unit 2				
	N-S Sections	23.2	0.72	7
	E-W Sections	23.2	0.84	8
Total - All Outcrops		Avg.	Std. Dev.	n
	N-S Sections	19.7	4.65	45
	E-W Sections	19.8	4.63	47

Table 10: Image Analysis Porosity; Directional Comparison of Horizontal and Vertical Thin Sections

	Horizontal Sections	Vertical Sections
Outcrop 1-Bedding Unit 1		
sample 1-10	11.8	14.5
Outcrop 2-Bedding Unit 1a		
sample 3-18	16.7	19.5
sample 3-30	15.0	18.1
-Bedding Unit 1b		
sample 5-12	13.6	22.3
sample 5-15	16.9	22.0
-Bedding Unit 2		
sample 6-6	21.6	20.2
sample 6-25	18.1	24.0
Outcrop 3-Bedding Unit 1		
sample 2-2	25.8	26.0
sample 2-5	23.6	24.0
-Bedding Unit 2		
sample 4-2	22.2	23.3
sample 4-8	19.1	22.7
Total - All Outcrops	18.7 s=3.73 n=11	21.5 s=3.08 n=11

Calculations using data from Table 5 demonstrate that within bedding units no statistical difference is present for mean values of percent presolved quartz. Outcrop mean values are also not statistically different at the 95% confidence level by t-test.

MECHANICAL POROSITY REDUCTION

Porosities upon deposition of well-sorted beach and dune sands, inferred to be the depositional environment of the Galesville Sandstone, are found to average approximately 49% (Pryor, 1973). The loose-packed Galesville sands compare favorably with this, having a mean porosity of 46.2%. Reduction in sandstone porosity begins shortly after burial by mechanical re-adjustment of grains into a more tightly packed arrangement. Mechanical compaction is prompted by pressure from loading and possibly minor earth movements. Compaction by mechanical re-adjustments tends to proceed until a stable grain framework is achieved, or until cementation by authigenic minerals makes intergranular movements impossible. The minimum porosity value established for tight packing of well-sorted and well-rounded sands in laboratory experiments is approximately 36% (Fraser, 1935; Gaither, 1953).

Two separate experiments were performed on disaggregated Galesville sands to determine the minimum possible porosity value due to mechanical compaction of the Galesville. Results from thin section analysis of Galesville

sands, artificially packed in the laboratory and impregnated, are listed in Table 11. The porosities resulting from three different packing techniques were determined by image analysis of four thin sections per packing arrangement. The second method of establishing porosity in the loose sands was performed by packing Galesville sands into a volumetric cylinder and determining porosity by volume-density calculations (Table 12).

Thin sections show an average maximum porosity reducation by mechanical compaction to approximately 35%. Volume-density determinations show porosity reduction to approximately 36%. Results for the two methods of porosity analysis are very similar to those established by previous work (Fraser, 1935). However, porosities as low as 33% were achieved by packing of Galesville sands in methanol while being tamped and ultrasonically treated.

This special method of compacting disaggregated sands demonstrates the possibility of reduction in randomly packed sands to near 33%. While conditions in the laboratory porosity reduction experiments using methanol and ultrasonic treatments are not comparable to conditions in natural sands; the special treatment may, in effect, accelerate mechanical compaction processes which occur in the natural environment over long periods of time.

A long period of mechanical grain adjustment during the early diagenetic history of the Galesville is suggested

Table 11: Image Analysis of Disaggregated Galesville Sandstone Thin Sections

I. Unpacked Sands

Sample #	% Porosity	Std. Dev.	n
5-5 L-A-1	43.1	2.74	36
5-5 L-A-2	42.9	2.72	36
3-29 L-A-1	42.2	1.98	36
3-29 L-A-2	45.2	2.18	36
Mean Porosity =	43.4	1.29	4

II. Sands Settled by Shaking

Sample #	% Porosity	Std. Dev.	n
5-5 L-B-1	38.0	2.82	36
5-5 L-B-2	37.9	2.63	36
3-29 L-B-1	35.9	2.24	36
3-29 L-B-2	36.3	2.54	36
Mean Porosity =	37.0	1.08	4

III. Sands Shaken and Tamped

Sample #	% Porosity	Std. Dev.	n
5-5 L-C-1	35.6	2.68	36
5-5 L-C-2	35.8	2.60	36
3-29 L-C-1	34.3	2.49	36
3-29 L-C-2	33.7	2.38	36
Mean Porosity =	34.9	1.01	4

Table 12: Porosity of Disaggregated Galesville Sands Determined by Volume - Density Analyses

I. Unpacked Sands:	% Porosity
	45.4
	54.7
	47.7
	45.9
	46.2
	46.1
Mean Porosity=	46.2

II. Sands Settled by Shaking:	% Porosity
	37.9
	38.5
	38.4
Mean Porosity=	38.3

III. Shaken and Tamped Sands:	% Porosity
	36.4
	36.0
	36.1
Mean Porosity=	36.2

IV. Sands in Methanol, Tamped, Ultrasonically Treated:	% Porosity
	33.0
	32.8
	33.1
Mean Porosity=	33.0

by very similar minus cement porosities and percentages of intergranular pressure solution for all outcrops, despite the variability in the quantity of quartz cement. If quartz cementation preceeded mechanical compaction, minus cement porosities at outcrops one and two would be significantly higher than outcrop three where cementation has not occurred.

PRESSURE SOLUTION

In addition to mechanical grain adjustments, intergranular pressure solution in the Galesville Sandstone has also occurred prior to authigenic quartz cementation. Nearly equivalent volumes of presolved detrital quartz at all outcrops measured would not be observed if cementation had occurred before, or synchronously with pressure solution. Authigenic cement would have stabilized grain contacts and reduced the percentage of presolved quartz where precipitated.

Pressure solution in the Galesville Sandstone is entirely intergranular in nature; no stylolitic development is observed in thin section or at the outcrop. Intergranular pressure solution is virtually undetectable under a normal petrographic microscope in the quartz cemented samples. An estimate of the volume of presolved quartz in the Galesville could only be made by cathodo-luminescence microscopy. Pressure solution relationships by petrographic

examination are less than obvious because of the small volume presolved and because very few sutured contacts are present.

MODELING POROSITY REDUCTION DUE TO PRESSURE SOLUTION

The porosity reduction in quartz arenites due to pressure solution between grains has been investigated by Rittenhouse (1971). He presents a theoretical model where spheres arranged in an orthorhombic lattice are compacted due to "overburden" pressure. As the volume of the lattice is decreased by vertical shortening, an overlap, or "solution" of the spheres occurs at points of contact throughout the lattice. The percent porosity reduction with pressure solution for the orthorhombic and other models are plotted on Figure 6.

The orthorhombic arrangement was chosen by Rittenhouse because of the close approximation of porosity in this lattice (39.54%, Graton and Fraser, 1935) to porosities observed in laboratory experiments with randomly packed sheres (Fraser, 1935, p. 936). The number of contacts per grain (8) also closely approximates the 7.5 contacts per sphere found in randomly packed lead shot (Marvin, 1939). Rittenhouse assumed that below 39.54%, porosity reduction would proceed only with pressure solution and/or cementation.

Since it is possible that pressure solution may begin in the Galesville at porosities below 39.54%, the relation between porosity reduction and pressure solution in a

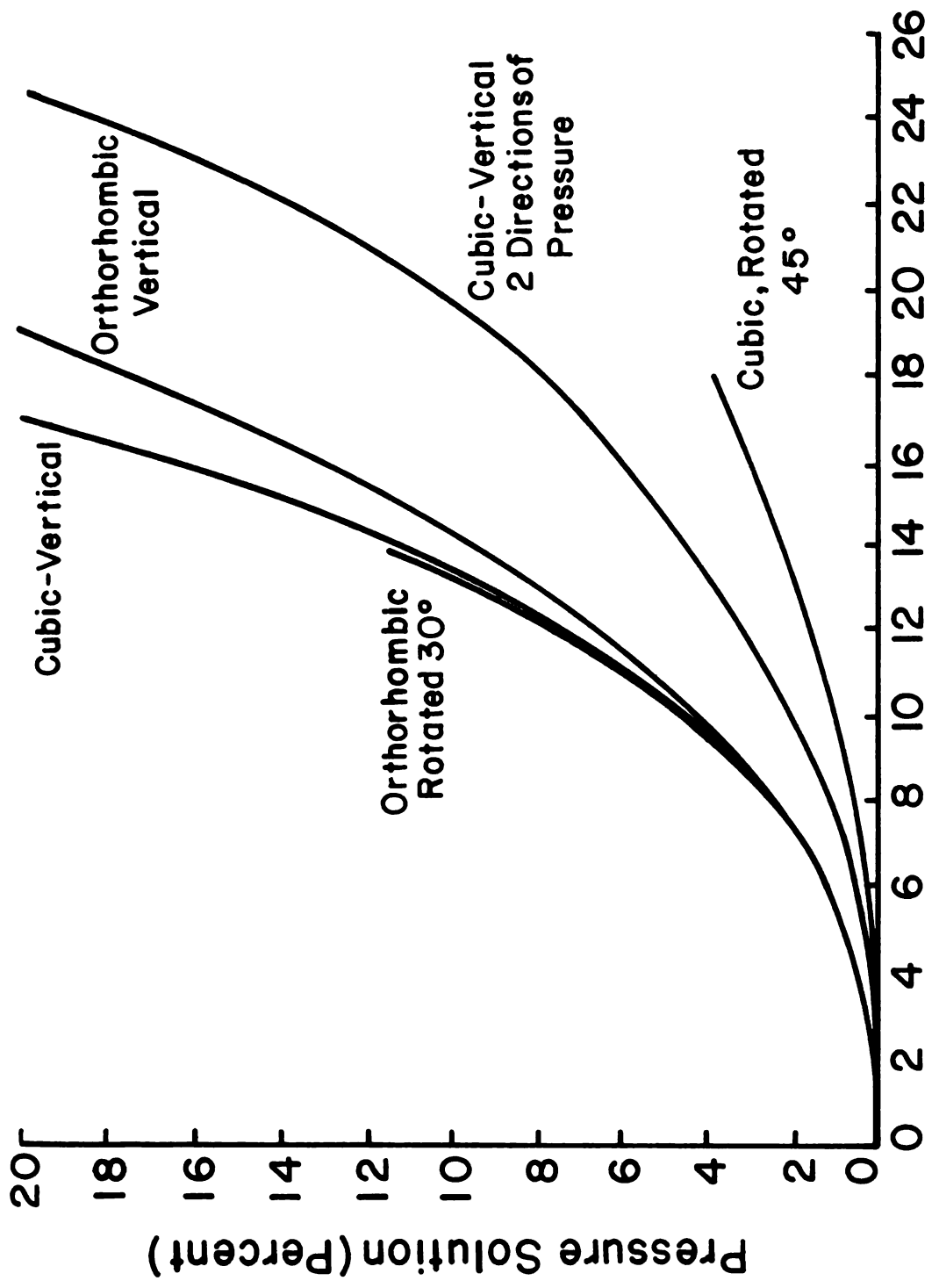

Figure 6--Porosity Reduction Due to Pressure Solution for Five Packing Arrangements of Spheres (After Rittenhouse 1971)

hexagonal close-packed arrangement of spheres was determined to establish the effect of a closer packed framework on the solution-reduction ratio. Porosity reduction was performed in a manner similar to that used by Rittenhouse for orthorhombic packing. A unit cell (Graton and Fraser, 1935, p. 800-804) was chosen and used as representative of porosity and grain relationships throughout the hexagonal lattice.

The unit cell is best described as a rhombohedron whose corners lie at the centers of eight adjacent spheres in the hexagonal lattice (see Figure 7). The orientation of the unit cell in relation to the direction of shortening was chosen to maximize the percentage porosity reduction with compaction. The mechanics of the model and the method of calculation are explained in Appendix B. Results show the pressure solution: porosity reduction ratio for hexagonally close-packed spheres is slightly higher than that calculated by Rittenhouse for orthorhombic-rotated 30 degrees and cubic-vertical arrangements. However, the results for these four packing arrangements are not drastically different and the pressure solution: porosity reduction ratios are comparable.

RELATIONSHIP BETWEEN MECHANICAL POROSITY REDUCTION AND REDUCTION BY PRESSURE SOLUTION

In the Galesville Sandstone, if mechanical compaction to minimum porosity values has occurred (to 33%), an

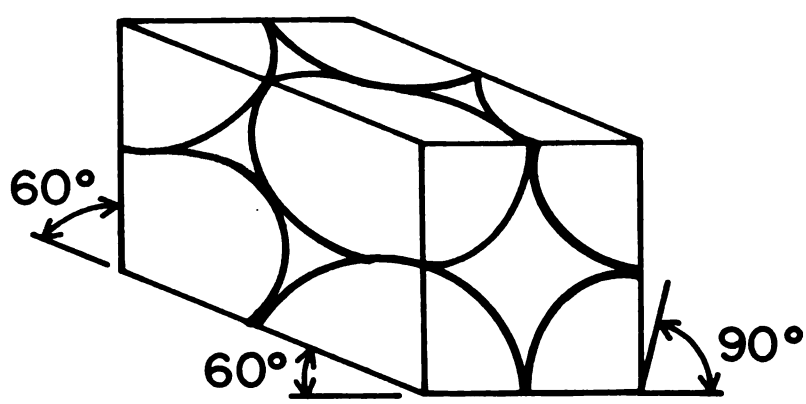

Figure 7--Unit Cell of A Hexagonal Lattice

additional 9% porosity reduction is required to reduce the minus cement of the measured 24%. The reduction of 9% below maximum mechanical porosity reduction is caused by intergranular pressure solution. Petrographic and luminescence analysis show that fracturing of grains is unimportant in the Galesville. No other process besides intergranular pressure solution is known which could reduce the cement porosity belwo that established for maximum mechanical adjustment (approximately 33%). The presolved volume of quartz responsible for the 9% porosity loss has been determined by point counts to be less than 1%. This pressure solution: porosity reduction ratio is significantly smaller than predicted from theoretical packing models. The smaller solutions: reduction ratio is due to the random rather than regular packing of grains and the imperfect grain shape and sorting characteristics of natural sands. The Galesville pressure solution: prrosity reduction ratio is shown in Figure 8 and compared with ratios for hexagonal and orthorhombic arrangements of spheres.

An additional consideration in porosity reduction during pressure solution is that a definite boundary does not exist between mechanical adjustment effects and reduction due to pressure solution in uncemented sands. The small scale displacements due to pressure solution at stressed grain contacts could conceivable affect grain packing and result in re-packing of grains mechanically.

Evidence supporting this possibility lies in the extreme friability of outcrops sampled. At outcrop three, uncemented

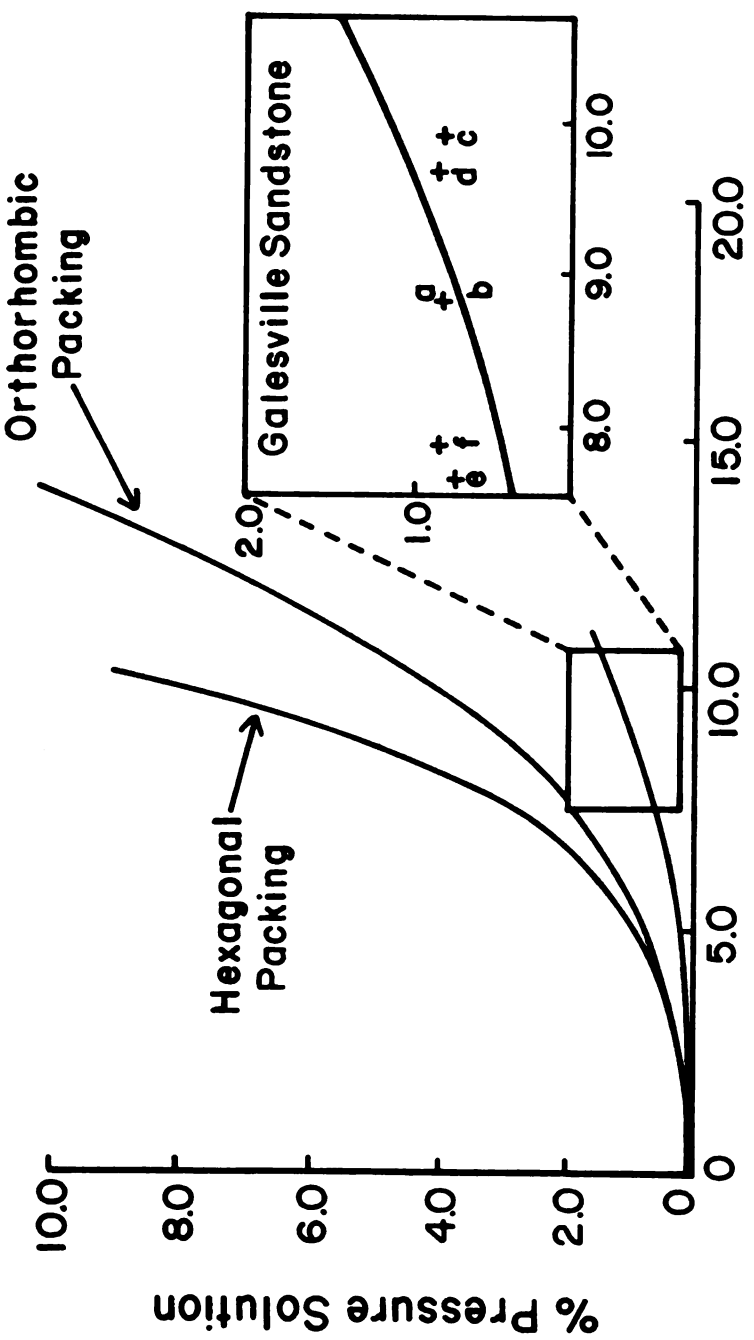

Figure 8--Pressure Solution to Porosity Reduction Relationships

sands having a porosity of 23.6% are easily crumbled under the slightest pressure. Presolved contacts in the sand do not act as cemented contacts. Mechanical re-packing of grains in this type of sand during early stages of pressure solution would not be hindered by cementation or coherence at presolved contacts.

Further evidence that mechanical re-packing proceeds with pressure solution lies in many observations of a "puzzle fit" of previously presolved contacts, now separated slight distances by void space or cement. This may occur if early presolved quartz contacts have been affected by mechanical adjustments even on a very small scale, causing re-packing and a change in the position of previous grain contacts.

As presolved intergranular contacts become more abundant in the sand with increasing depth of burial, the grain framework tends to become more and more stablized. As a result, the importance of mechanical adjustments will be rapidly decreased as pressure solution proceeds.

Since adjustment and separation of presolved grain contacts has occurred in the Galesville, the actual percentage of presolved quartz will be slightly higher than that estimated by measuring the areas of interpenetration at grain contacts. The difference in these values, however, is not significant. Presolved grain contacts which have since been separated are often noticable under cathodoluminescence. The volume presolved, however, is not of significance when compared with the greater (approximately

40X) volume of presolved quartz occurring at interpenetrating grain contacts.

LARGE SCALE EFFECTS OF POROSITY REDUCTION

Geologic and structural maps of the Baraboo syncline area (Hanson, 1970; Thwaites, 1935, p. 393) show a gentle structural depresssion of the upper contact of the Galesville Sandstone. Nearly 150 feet of relief is present, from the margin of the Baraboo Syncline deepening into the center. This depression is not due to folding since deformation forming the structure of the syncline's metamorphic rocks is of Precambrain age.

It has been suggested that the structurally higher position of the Galesville sands around the Baraboo cliffs may be due to conditions during sandstone deposition. In a higher energy beach environment around the cliffs, thick sands were deposited. If these graded to finer sediments deeper within the syncline, it is possible that the contact observed and mapped is a result of the paleoslope into the syncline and/or a change in facies to finer-grained sediments within the syncline.

Another possible factor in the structural depression is the differential compaction of the sediments (Hedberg, 1926), from a thick sedimentary column in the center, thinning and onlapping the quartzite around the margins. An estimate of the possible effect of differential compaction

can be calculated by multiplying the depth to bedrock within the syncline by the fractional reduction in volume due to compaction of the sedimentary column below the Galesville.

A volume reduction of approximately 25% has occurred within the Galesville from an initial depositional porosity of 49% to the detrital grain porosity of approximately 24% measured in thin sections. The degree of porosity reduction and compaction of the Galesville provides a good basis for the porosity loss expected in the underlying column which is predominantly sandstone to bedrock. The actual vertical compaction calculated is a maximum since compaction began in the underlying units before Galesville deposition.

Depths to bedrock in the syncline have been reported by Weidman (1904) from drilling of water wells. He records depths of over 560 feet from wells close to the deepest part of the syncline. Using these figures, a maximum estimate of 0.25 x 560 feet, or 140 feet, difference in elevation may have resulted form differential compaction. It is concluded from this estimate that compaction was a major factor in producing the present structural configuration of the Galesville Sandstone.

CONCLUSIONS

1) Porosity reduction in the Galesville Sandstone is determined to be due to three factors. These are:

   a) Up to 16% porosity reduction by mechanical grain adjustments.

b) A minimum of 9% porosity reduction after the onset of intergranular pressure solution.

c) Implacement of variable quantities of quartz (0-4.5%), adularia (0-0.9%, kaolinite, and iron oxides and hydroxides after the completion of grain adjustments and pressure solution.

2) Intergranular pressure solution in natural sands results in significantly lower pressure solution: porosity reduction ratios than demonstrated by theoretical models using packing arrangements of perfect spheres.

3) During early stages of pressure solution, additional porosity reduction may result from accompanying grain adjustments in uncemented sands.

4) The volume of authigenically precipitated quartz cement in the Galesville Sandstone is unrelated to the percent intergranular pressure solution.

5) Large variations in minus cement porosity and percent pressure solution only occur on a very small scale within the the Galesville Sandstone. Variation within thin sections is greater than that observed between thin sections, beding units and outcrops.

6) Differences in porosity according to thin section orientation are not statistically significant in the Galesville Sandstone.

7) Intergranular pressure solution, virtually undetectable under a normal petrographic microscope, can have a significant effect on porosity reduction in sandstones.

8) The differential compaction of sediments within the Baraboo Syncline is a major factor in the development of the present structural configuration of the Galesville-Tunnel City contact.

RECOMMENDATIONS FOR FURTHER STUDY

At the present time, little precise knowledge exists concerning the effect of pressure solution on porosity reduction in natural, randomly-packed sands. Laboratory experiments using apparatus designed to evaluate the effect of porosity reduction with pressure solution would be very useful by helping to define the relative importance of mechanical and chemical processes on the reduction in pore space.

Other useful lines of research involving the mode of porosity reduction in sandstones could include: 1). Evaluation of the diagenetic effects on clean quartzose sandstones which have undergone greater depths of burial 2). Evaluation of the effect of differing sandstone compositions on diagenetic porosity reduction with increasing depths of burial.

Work toward an understanding of the relative importance of variables able to be isolated for observation in compositionally and texturally simplistic sandstones can lead toward a better understanding of the diagenetic alteration and porosity reduction which occurs in natural sandstones.

BIBLIOGRAPHY

BIBLIOGRAPHY

Chayes, F., 1956, Petrographic Model Analysis: An Elementary Statistical Appraisal: John Wiley and Sons, Inc., New York.

Chung, P.K., 1973, Mississippian Coldwater Formation of the Michigan Basin: Ph.D. Thesis, Michigan State University.

Cohee, G.V., 1948, Cambrian and Ordovician Rocks in Michigan and Adjoining Areas: Am. Assoc. Petroleum Geologists Bull., v. 32, no. 8, pt. 2, p. 1417-1448.

Dalziel, I.W.S., Dott, R.H. Jr., and Black, R.F., 1970, Geology of the Baraboo District, Wisconsin: University of Wisconsin, Geological and Natural History Survey, Information Circular #14, p. 39-41.

Driscoll, E.G., 1959, Evidence of Transgressive-Regressive Cambrian Sandstones Bordering Lake Superior: Jour. Sed. Petrology, v. 29, p. 5-15.

Emrich, G.H., 1966, Ironton and Galesville Sandstones in Illinois and Adjacent Areas: Ill. State Geology Survey, Circular 43o, p. 55.

Fraser, H.J., 1935, Experimental Study of the Porosity and Permeability of Clastic Sediments: Jour. Geology, v. 43, p. 910-1010.

Friedman, G.M., 1961, Determination of Sieve-Size Distributing from Thin Section Data for Sedimentary Petrological Studies: Jour. Geology, v. 66, p. 394-416.

Gaither, A., 1953, A study of the Porosity and Grain Relationships in Experimental Sands: Jour. Sed. Petrology, v. 23, p. 180-195.

Graton, L.C. and Fraser, H.J., 1935, Systematic Packing of Spheres with Particular Relation to Porosity and Permeability: Jour. Geology, v. 43, p. 785-909.

Hamblin, W.K., 1961, Paleogeographic Evolution of the Lake Superior Region: Geol. Soc. America Bull., v. 72, p. 1-18.

Hanson, G.F., 1970, Geologic Map of the Baraboo District: University of Wisconsin, Geological and Natural History Survey.

Hedberg, H.D., 1926, The Effect of Gravitational Compaction on the Structure of Sedimentary Rocks: Am. Assoc. Petroleum Geolobists Bull., v. 10, p. 1035-1072.

Kansas Geological Society Guidebook, 1935, Ninth Annual Field Conference, Upper Mississippi Valley.

Marvin, J.W., 1939, The Shape of Compressed Lead Shot and its Relation to Cell Shape: American Journal of Botany, v. 26, p. 288-295.

Melhorn, W.N., 1958, Structural Analysis of Silurian Rocks in the Michigan Basin: Am. Assoc, Petroleum Geologists Bull., v. 42, p. 816-838.

Minoura, N. and Conley, C.D., 1971, Technique for Impregnating Porous Rock Samples with Low-Viscosity Epoxy Resin: Jour. Sed. Petrology, v. 41, p. 858-861.

Ostrom, M.E., 1966, Cambrian Stratigraphy in W. Wisconsin: University of Wisconsin, Geological and Natural History Survey, Information Circular #7.

_____1967, Paleozoic Nomenclature for Wisconsin: University of Wisconsin, Geological and Natural History Survey, Information Circular #8.

Pryor, W.A., 1973, Permeability-Porosity Patterns and Variations in Some Holocene Sand Bodies: Am. Assoc. Petroleum Geologists Bull., v. 57, p. 162-189.

Raasch, G.O., 1935, Paleozoic Strata of the Baraboo Area: In Guidebook, Ninth Annual Field Conference, Kansas Geological Society.

Rittenhouse, G., 1971, Pore-Space Reduction by Solution and Cementation: Am. Assoc. Petroleum Geologists Bull., v. 55, p. 80-91.

Rutgers, R., 1962, Packing of Spheres: Nature, v. 193, p.465-466.

Schuchert, C., 1955, Atlas of Paleogeographic Maps of North America: John Wiley and Sons, Inc., New York.

Scott, G.D., 1960, Packing of Equal Spheres: Nature, v. 188, p. 908-909.

Sippel, R.F., 1968, Sandstone Petrology, Evidence from Luminescence Petrography: Jour. Sed. Petrology, v. 38, p. 530-554.

Thwaites, F.T., 1930, Buried Pre-Cambrian of Wisconsin: Geol. Soc. America Bull., v. 42, p.719-750.

_____1935, Physiography of the Baraboo District, Wisconsin: in Kansas Geological Society, Ninth Annual Field Conference Guidebook

Twenhofel, W.H., 1935, Cambrian Strata of Wisconsin: Geol. Soc. America Bull., v. 46, p. 1687-1744.

Weidman, S., 1904, The Baraboo Iron Bearing District of Wisconsin: University of Wisconsin Geological and Natural History Survey, Bull. 13.

Wanenmacher, J.M., Twenhofel, W.H., and Raasch, G.O., 1934, Paleozoic Strata of the Baraboo Area, Wisconsin: American Journal of Science, v. 228, p. 1-30.

Willman, H. B., et al, 1975, Handbook of Illinois Stratigraphy: Illinois State Geological Survey, Bull. #95.

APPENDIX A

APPENDIX A

DESCRIPTION OF SAMPLING LOCATIONS.

Outcrop One: One bedding unit sampled

Location: NE NW S32 T12N R5E. Galesville outcropping in flagstone quarry 0.6 miles west of the intersection of highways 136 and 154 in Rock Springs. Outcrop one is located on the synclinal margin, deposited within a erosional break in the quartzite.

The Galesville Sandstone at this location displays large festoon cross stratification. Troughs range from 20 to 60 feet wide, up to 40 feet in length and have a typical amplitude to 2 to 3 feet. The sandstone is unusually well indurated. Cement includes authigenic quartz with minor hematite. Variable amounts of kaolinite and iron oxide are present interstitially. Detrital quartz grains are well-rounded and well-sorted, of medium sand size. Abundant dust rings are observable in thin section.

Outcrop Two: Two bedding units sampled.

Location: NE SE S16 T11N R5E. La Rue quarry, 100 feet South of LaRue city limits on highway PF. Outcrop two is located inside the Baraboo syncline. Bedding unit one was sampled in two locations (1a and 1b), located approximately twenty feet laterally. Bedding unit two was located approximately 15 feet stratigraphically below unit one. Bedding units were composed of massive sands internally unstructured

and unlaminated. Bedding units sampled were defined by differences in weathering characteristics on the outcrop face.

The Galesville is a very clean quartz sandstone at this location. Quartz cement varies from 1.7% to 4.3% between sampling grids. Some minor hematite is present in the upper section of the quarry from weathering in the overlying soil horizon. Detrital quartz grains for all grids measured are well-rounded and well-sorted, medium sand sized.

Authigenic adularia composing up to 1% of the rock volume is found in the interstices of the sandstone. Crystals of adularia by microprobe analysis contain greater than 99% potassium. Adularia has precipitated in the pore spaces of the Galesville without detrital feldspar cores. Crystals have a characteristic rhombahedrla form, low relief and low birefringence. Adularia displays a dull green luminescence.

Outcrop Three: Two bedding units sampled.

Location: NW SW S13 T10N R5E. Outcrop on hill, one mile north of junction to Denzer on highway C, 200 feet east of road. Outcrop three is located outside of the Baraboo Syncline.

Both bedding units sampled consisted of massive, extremely friable quartz sands. Sands contained a small percentage of fine silt composed of quartz and detrital feldspar. Microprobe analysis shows the feldspars to be potassium feldspar, 96% to 98% potassium. Bedding unit one is approximately 20 feet stratigraphically higher than bedding unit two, separated by a less resistant bench former of finer grained sandstone-siltstone.

The detrital feldspar fraction is very visable under cathodo-luminescence due to its bright blue luminescent quality. Authigenic feldspar overgrowths are present; however, large euhedral feldspar crystals are not present as in Outcrop #2.

Quartz grains exhibit primary rounded shapes. No quartz cement is present at this outcrop. Grains are well-rounded and well-sorted of medium sand size. The small quantity of detrital silt grains are for the most part not visable in thin section under plane light because the fine grains are most often submersed in the red epoxy.

APPENDIX B

APPENDIX B

POROSITY REDUCTION DUE TO PRESSURE SOLUTION IN HEXAGONALLY CLOSE-PACKED SPHERES

As vertical compaction of the hexagonal close-packed model proceeds, interpenetration of grains occurs at point contacts as depicted in the cross section, Figure 9. Horizontal displacement or rotation of spheres does not occur within the model during compaction.

The volume of interpenetration is equal at all contacts and can be calculated by using the equation for the volume of a spherical segment.

$$V_{(segment)} = 1/3\pi h^2 \ (3r-h)$$

Within each unit cell there are a total of two spherical segments where interpenetration occurs.

When compaction from A to A' causes displacement x as in Figure 9, the length of h can be calculated by subtracting the length of the line connecting the centers of two interpenetrating spheres from the length of the line before compaction.

$$h = 2-\sqrt{[(8/3)^{1/2} - x]^2 + (4/3)}$$

The total volume of the unit cell is equal to the area of the base times the height. With increasing compaction, the volume of the rhombohedron is defined by the equation:

$$V_{rhomb} = 3.464 \ (\sqrt{8/3} - x)$$

The pore space within the hexagonal lattice is determined by subtracting the volume of the two spherical segments from

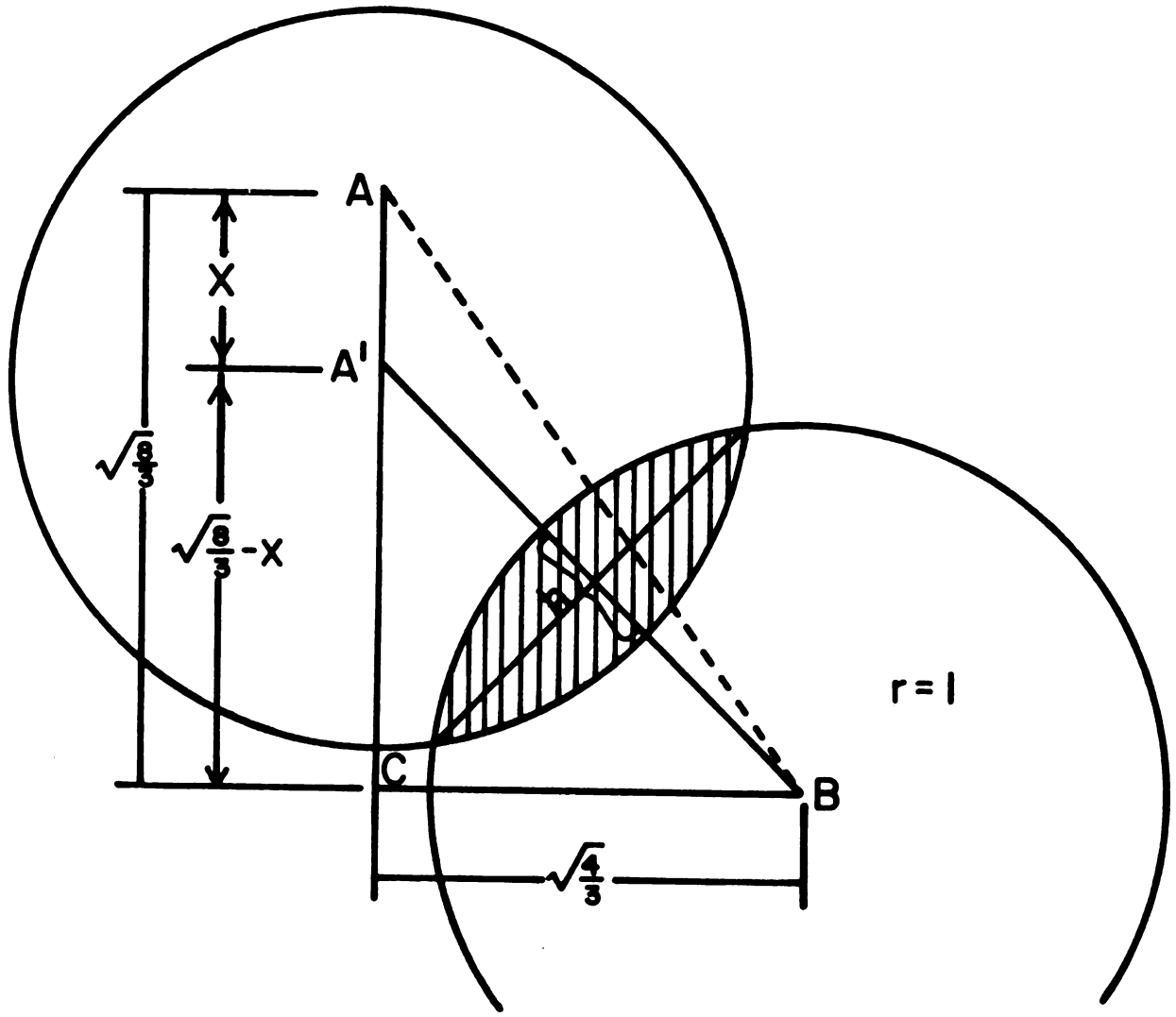

Figure 9--Pressure Solution Relationships During Vertical Compaction of the Hexagonal Model

the volume of the spheres and then subtracting that total from the volume of the rhombohedron. The percent porosity is obtained by dividing the volume of pore space by the volume of the rhombohedron and multiplying by 100. The expression may be used:

$$\% \text{ Porosity} = 100 \left[\frac{[3.464(\ 8/3 - x) - 4/3\pi r^2 - 2/3\pi h^2(3r-h)]}{3.464(\ 8/3 - x)} \right]$$

The percent volume of the unit cell which has been overlapped or presolved at the points of contact is determined by calculating the volume of the spherical segments within the unit cell, dividing this by the volume of the rhombohedron and multiplying by 100. The expression may be used:

$$\% \text{ Pressure Solution} = 100 \left[\frac{2/3\pi h^2(3r-h)}{3.464(\ 8/3 - x)} \right]$$

Making use of the equations formulated above, Table 13 and Figure 10 were prepared.

The plus cement porosity assumes that material presolved at point contacts further decreases porosity by being precipitated within the model as cement. Minus cement porosity is the porosity of the spheres subtracting the effects of any precipitation of dissolved material.

Table 13: Compaction of a Hexagonal Close-Packed Arrangement of Sheres

% Compaction	% Pressure Solution	Minus Cement Porosity	Porosity Reduction	Plus Cement Porosity	Porosity Reduction
0	0	25.95	0	25.95	0
5	0.50	22.55	3.44	22.05	3.90
10	2.02	19.75	6.62	17.73	8.22
15	4.61	17.51	8.48	12.90	13.05
20	8.40	15.79	10.20	7.39	18.56

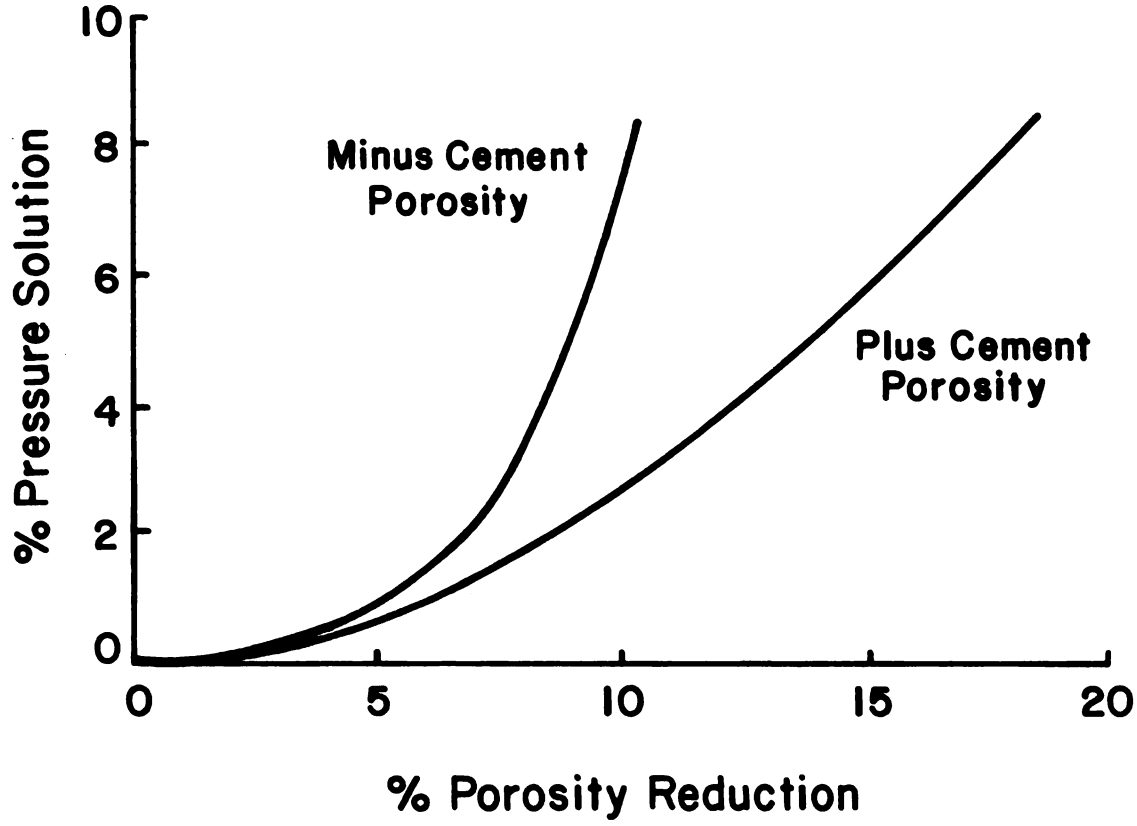

Figure 10--Percent Pressure Solution Versus Percent Porosity Reduction for Hexagonally Close-Packed Spheres

APPENDIX C

IMAGE ANALYSIS AND POINT COUNTS OF CATHODO-LUMINESCENCE MICROSCOPE PHOTOGRAPHS

RESULTS: Point Counts, Outcrop #1, Bedding Unit #1

Slide	Grain	Over-growth	Total	Pressure Solution	% Porosity Image Analysis		% Adularia	% Quartz Cement	% Pressure Solution	% Porosity Minus Cement
					%	S				
1-EN	258.5	23.5	282.0	6.0	11.2	2.61	0.0	7.4	1.9	18.6
1-EN	439.5	13.0	452.5	3.5	11.2			2.6	0.7	13.8
1-EE	453.0	15.0	468.0	13.5	13.8	2.81		2.8	2.5	16.6
1-EE	678.0	20.0	698.0	8.5	13.8			2.5	1.0	16.3
1-FD	394.0	23.5	417.5	3.5	14.8	3.23		4.9	0.7	19.7
1-FD	479.0	27.5	506.5	10.0	14.8			4.6	1.7	19.4
1-FS	330.0	11.5	341.5	3.5	16.1	2.71		2.8	0.9	19.0
1-FS	152.5	4.5	157.0	0.0	16.1			2.4	0.0	18.5
1-6N	269.5	11.0	280.5	2.5	12.2	2.60		3.4	0.8	15.6
1-6N	532.5	49.5	582.0	9.0	12.2			7.5	1.4	19.7
1-7N	196.5	12.0	208.5	0.0	11.4	4.58		5.1	0.0	16.5
1-7N	409.5	9.5	419.0	6.5	11.4			2.0	1.4	13.4
1-8N	328.5	27.0	355.5	0.0	13.2	2.94		6.6	0.0	19.8
1-8N	218.5	7.0	225.5	0.0	13.2			2.7	0.0	15.9
1-8E	352.0	15.0	367.0	1.0	8.7	2.69		3.7	0.2	12.4
1-8E	400.5	27.5	428.0	4.0	8.7			5.9	0.9	14.6
1-8E	451.5	21.0	472.5	0.0	8.7			4.1	0.0	12.8
1-6E	640.5	42.0	682.5	5.0	11.4	2.68		5.5	0.6	16.9
1-6E	211.5	5.5	217.0	2.0	11.4			2.2	0.8	13.6
1-10Nb	416.5	32.5	449.0	4.0	14.9	3.44		6.2	0.8	21.1
1-10Nb	339.5	16.5	356.0	3.5	14.9			3.9	0.8	18.8
1-10E	655.0	35.0	690.0	3.0	14.0	3.53		4.4	0.3	18.4
1-10E	645.5	43.0	688.5	7.5	14.0			5.4	0.9	19.4
1-12N	470.5	38.5	509.0	8.5	16.0	3.15		6.4	1.4	22.4
1-12N	228.0	12.5	240.5	3.0	16.0			4.4	1.0	20.4
1-12E	311.5	14.5	326.0	8.0	15.8	3.08		3.7	2.1	19.5
1-12E	572.0	40.5	612.5	8.5	15.8			5.6	1.2	21.4

RESULTS: Point Counts, Outcrop #1, Bedding Unit #1 continued

Slide	Grain	Over-growth	Total	Pressure Solution	% Porosity Image Analysis		% Adularia	% Quartz Cement	% Pressure Solution	% Porosity Minus Cement
					$\bar{x}$ %	S				
1-13Na	397.0	48.5	445.5	0.0	12.0	2.52	0.0	9.6	0.0	21.6
1-13Na	743.0	42.5	785.5	6.5	12.0			4.8	0.7	16.8
1-13Nb	173.0	12.5	185.5	5.0	14.4	2.42		5.8	2.3	20.2
1-13Nb	219.0	7.0	226.0	1.0	14.4			2.7	0.4	17.1
1-18N	90.5	5.0	95.5	0.0	10.2	2.26		4.7	0.0	14.9
1-18N	462.0	11.5	473.5	2.5	10.2			2.2	0.5	12.4
1-18E	762.0	37.5	799.0	4.0	10.0	2.20		4.2	0.5	14.2
1-18E	255.5	7.0	273.5	5.5	10.0			2.2	1.8	12.2
1-19N	447.5	32.0	479.5	4.0	11.9	4.17		5.8	0.7	17.7
1-19N	396.0	32.0	428.0	3.5	11.9			6.5	0.7	18.4
1-19E	424.5	31.5	456.0	6.0	10.5	2.25		6.0	1.2	16.5
1-19E	216.0	19.0	235.0	2.5	10.5			7.0	1.0	17.5
1-22N	563.0	31.5	594.5	4.0	12.5	2.21		4.6	0.6	17.1
1-22N	704.5	47.5	752.0	0.0	12.5			5.5	0.0	18.0
1-22E	294.0	14.5	308.5	1.5	11.2	2.64		4.1	0.4	15.3
1-22E	396.5	28.5	425.0	1.5	11.2			5.8	0.3	17.0
1-7E	104.0	25.5	129.5	2.0	13.7	3.24		17.2	1.3	30.9
1-7E	419.0	34.5	453.5	1.0	13.7			6.6	0.2	20.3
1-13E	233.5	9.5	243.0	0.0	11.8	3.06		3.4	0.0	15.2
	18145.5	1075.5	19221.0	175.0	12.8% (s=2.05) (n=23)		0.0%	4.89% (s=2.77) (n=46)	0.80% (s=0.65) (n=46)	17.5% (s=3.34) (n=46)

RESULTS: Point Counts, Outcrop 3, Bedding Unit 1

Slide	Total	Pressure Solution	% Porosity Image Analysis		% Adularia	% Quartz Cement	% Pressure Solution	% Porosity Minus Cement
			%	S				
2-1N	1855	17.5	22.0	3.46	0.0	0.0	0.9	22.0
2-1N	1855	12.0	22.0				0.6	22.0
2-1E	1855	19.5	24.6	3.40			1.1	24.6
2-1E	1855	14.0	24.6				0.8	24.6
2-2N	1855	4.0	25.9	2.51			0.2	25.9
2-2N	1855	13.5	25.9				0.7	25.9
2-2E	1855	22.5	26.1	2.89			1.2	26.1
2-2E	1855	14.0	26.1				0.8	26.1
2-3N	1855	16.0	25.0	2.73			0.9	25.0
2-3N	1855	9.0	25.0				0.5	25.0
2-3E	1855	13.0	23.6	3.34			0.7	23.6
2-3E	1855	6.5	23.6				0.4	23.6
2-4E	1855	23.5	21.1	4.24			1.3	21.1
2-4E	1855	14.0	21.1				0.8	21.1
2-4N	1855	29.0	24.1	2.42			1.6	24.1
2-4N	1855	18.0	24.1				1.0	24.1
2-5E	1855	13.0	24.0	2.27			0.7	24.0
2-5E	1855	10.5	24.0				0.6	24.0
2-9N	1855	24.0	26.5	2.87			1.3	26.5
2-9N	1855	30.5	26.5				1.6	26.5
2-9E	1855	23.0	23.3	2.92			1.2	23.3
2-9E	1855	19.0	23.3				1.0	23.3
	40810	366.0	24.2% (s=1.64) (n=11)		0.0%	0.0%	0.90% (s=0.36) (n=22)	24.2% (s=1.64) (n=11)

RESULTS: Point Counts, Outcrop #2, Bedding Unit #1a

Slide	Grain	Over-growth	Total	Pressure Solution	% Porosity Image Analysis		% Adularia	% Quartz Cement	% Pressure Solution	% Porosity Minus Cement
					%	S				
3-6N	299.5	25.5	325.0	0.0	23.7	2.38	.42	6.0	0.0	30.1
3-6N	513.0	38.0	551.0	2.0	23.7		.34	5.3	0.3	32.4
3-6E	377.0	20.5	397.5	0.0	19.1	2.51	.16	4.2	0.0	23.5
3-6E	280.5	17.5	298.0	0.5	19.1		.27	4.7	0.1	24.1
3-8N	196.5	11.5	208.0	4.0	18.2	2.59	0.0	4.5	1.6	22.7
3-8N	259.0	21.0	280.0	5.5	18.2		1.27	6.1	1.6	25.6
3-8E	464.0	18.5	482.5	3.5	20.8	2.48	0.0	3.0	0.6	23.8
3-8E	263.0	14.0	277.0	3.0	20.8		0.0	4.0	0.9	24.8
3-16N	467.0	13.0	480.0	5.5	17.7	2.16	0.0	2.2	0.9	19.9
3-16N	233.5	5.0	238.5	4.0	17.7		0.0	1.7	1.4	19.4
3-18E	633.5	14.5	648.0	7.0	19.3	2.57	.37	1.8	0.9	21.5
3-18E	419.0	18.5	437.5	0.0	19.3		.08	3.4	0.0	22.8
3-18N	324.0	8.5	332.5	1.5	19.7	3.68	0.0	2.1	0.4	21.8
3-18N	504.5	45.5	550.0	11.0	19.7		.32	6.6	1.6	26.6
3-16E	163.5	10.0	173.5	3.5	20.6	1.91	.29	4.5	1.6	25.4
3-28N	233.0	5.0	238.0	0.5	19.9	2.25	.11	1.7	1.7	21.7
3-28N	310.5	4.0	314.5	5.5	19.9		.53	1.0	1.4	21.4
3-28E	608.0	20.0	628.0	10.0	17.8	1.73	.45	2.6	1.3	20.9
3-30N	238.0	8.5	246.5	0.0	18.2	1.82	.69	2.8	0.0	21.7
3-30N	350.5	18.0	368.5	2.0	18.2		.11	4.0	0.4	22.3
3-30E	173.5	14.0	178.5	2.0	17.9	2.71	0.0	6.1	6.1	24.0
3-30E	237.5	5.0	242.5	1.0	17.9		0.0	1.7	1.7	19.6
	7545.5	356.0	7904.5	72.0	19.4% (s=1.72) (n=11)		0.25% (s=0.31) (n=22)	3.6% (s=1.7) (n=22)	0.91% (s=0.63) (n=22)	23.3% (s=2.76) (n=22)

RESULTS: Point Counts, Outcrop 3, Bedding 2

Slide	Total	Pressure Solution	% Porosity Image Analysis		% Adularia	% Quartz Cement	% Pressrue Solution	% Porosity Minus Cement
			$\bar{x}$	S				
4-2Ea	1855	8.5	23.3	3.11	0.0	0.0	0.4	23.3
4-2Ea	1855	23.5	23.3				1.1	23.3
4-5N	1855	7.5	21.6	2.67			0.4	21.6
4-5N	1855	11.5	21.6				0.5	21.6
4-5E	1855	14.0	22.6	2.74			0.7	22.6
4-5E	1855	18.5	22.6				0.9	22.6
4-6N	1855	23.5	23.5	3.31			1.1	23.5
4-6E	1855	19.0	22.8	3.17			0.9	22.8
4-6E	1855	21.5	22.8				1.0	22.8
4-7N	1855	18.0	23.8	2.59			0.8	23.8
4-7N	1855	10.5	23.8				0.5	23.8
4-7E	1855	21.5	23.3	2.72			1.0	23.3
4-7E	1855	19.0	23.3				0.9	23.3
4-8N	1855	15.5	23.3	2.11			0.7	23.3
4-8N	1855	15.0	23.3				0.7	23.3
4-9N	1855	9.0	23.4	2.54			0.4	23.4
4-9N	1855	9.5	23.4				0.4	23.4
4-9E	1855	18.5	22.8	2.57			0.9	22.8
4-9E	1855	16.5	22.8				0.8	22.8
4-8E	1855	34.0	22.0	3.29			1.6	22.0
4-8E	1855	19.5	22.0				0.9	22.0
4-12N	1855	17.0	23.2	2.24			0.8	23.2
4-12N	1855	11.0	23.2				0.5	23.2
4-12E	1855	11.0	24.3	2.34			0.5	24.3
4-12E	1855	6.5	24.3				0.3	24.3
	46375	399.5	23.1% (s=0.70) (n=13)		0.0%	0.0%	0.86% (s=0.30) (n=25)	23.1% (s=0.70) (n=13)

RESLUTS: Point Counts, Outcrop #2, Bedding Unit 1b

Slide	Grain	Over-growth	Total	Pressure Solution	% Porosity Image	% Porosity Analysis	% Adularia	% Quartz Cement	% Pressure Solution	% Porosity Minus Cement
					%	S				
5-8E	39.5	3.0	42.5	0.0	20.6	2.20	0.0	5.6	0.0	26.2
5-8E	157.0	10.0	167.0	0.5	20.6		.43	4.8	0.2	25.8
5-8N	204.0	7.5	211.5	4.0	20.3	1.95	.46	2.8	1.5	23.6
5-8N	484.0	40.0	524.0	4.0	20.3		.86	6.1	0.6	27.3
5-11N	137.0	7.5	144.5	1.5	22.9	2.00	.43	4.0	0.8	27.3
5-11N	281.5	4.5	286.0	4.5	22.9		.46	1.2	1.2	24.6
5-11E	306.5	9.5	316.0	2.0	22.0	2.20	.49	2.3	0.4	24.8
5-11E	401.5	31.0	432.5	5.0	22.0		.51	5.6	0.9	28.1
5-12N	417.0	43.5	460.5	3.0	23.2	2.77	.11	7.3	0.5	30.6
5-12N	400.5	47.5	448.0	2.5	23.2		.67	8.1	0.4	32.0
5-12E	235.5	12.0	247.5	3.5	21.4	2.54	.86	3.8	1.1	26.1
5-12E	414.0	20.0	434.0	1.5	21.4		.57	3.6	0.3	25.6
5-13N	64.0	2.5	66.5	0.0	19.1	2.07	.32	3.0	0.0	22.4
5-13N	345.5	35.0	380.5	4.5	19.1		.35	7.4	1.0	26.9
5-13Ea	568.5	31.5	600.0	9.0	17.2	1.74	.19	4.3	1.2	21.7
5-13Ea	537.0	24.5	561.5	5.5	17.2		0.0	3.6	0.8	20.8
5-13Eb	290.5	11.0	301.5	1.5	20.1	1.70	.08	2.9	0.4	23.1
5-13Eb	527.0	31.5	558.5	6.5	20.1		.14	4.5	0.9	24.7
5-15N	345.0	18.5	363.5	3.5	21.5	2.22	.30	4.0	0.8	25.8
5-15N	376.0	13.5	389.5	2.5	21.5		0.0	2.7	0.5	24.2
5-15E	83.0	1.5	84.5	0.0	22.5	2.29	.05	1.4	0.0	24.0
5-15E	252.0	20.0	272.0	3.0	22.5		.03	5.7	0.9	28.2
5-19N	133.5	4.0	137.5	3.5	19.3	1.74	.57	2.3	2.1	22.2
5-19N	496.0	12.0	508.0	10.5	19.3		.19	1.9	1.7	21.4
5-22N	141.0	4.5	145.5	3.0	18.7	2.28	3.80	2.5	1.7	25.0
5-22N	102.5	1.0	103.5	1.0	18.7		.14	0.8	0.8	19.6
5-22E	291.5	14.0	305.5	2.0	20.4	2.29	1.38	3.6	0.5	25.4
5-22E	174.0	13.5	187.5	2.5	20.4		.84	5.7	1.1	26.9
	8205.0	474.5	8679.5	90.0	20.7% (s=1.69) (n=14)		0.53% (s=0.72) (n=28)	4.3% (s=1.91) (n=28)	0.82% (s=0.53) (n=28)	25.5% (s=2.823) (n=28)

RESULTS: Point Counts, Outcrop #2, Bedding Unit #2

Slide	Grain	Over-growth	Total	Pressure Solution	% Porosity Image Analysis		% Adularia	% Quartz Cement	% Pressure Solution	% Porosity Minus Cement
					$\bar{x}$	S				
6-6N	167.0	2.0	169.0	3.5	20.1	2.26	.53	0.9	1.7	21.5
6-6N	396.0	18.5	414.5	1.5	20.1		.11	3.6	0.3	23.3
6-6E	308.0	6.5	314.5	2.0	20.2	3.10	.64	1.6	0.5	22.4
6-6E	193.0	11.0	204.0	1.5	20.2		.42	4.3	0.6	24.9
6-20E	541.5	17.0	558.5	7.5	23.1	1.53	0.0	2.3	1.0	25.4
6-20E	332.5	4.0	336.5	1.5	23.1		.4	0.9	0.3	24.4
6-22E	238.0	7.0	245.0	1.5	19.9	2.07	1.25	2.3	0.5	23.5
6-22E	191.0	2.0	193.0	6.0	19.9		.40	0.8	1.6	21.1
6-23N	276.0	7.5	283.5	4.0	22.9	3.06	.32	2.0	1.1	25.2
6-23N	271.5	6.5	278.0	5.5	22.9		2.70	1.8	1.5	27.4
6-23E	329.0	4.5	333.5	2.0	22.9	2.87	.53	1.0	0.5	24.4
6-23E	279.0	6.5	285.5	2.0	22.9		2.26	1.8	0.5	27.0
6-24N	319.5	2.0	321.5	2.0	22.3	2.70	1.78	0.5	0.5	24.3
6-24N	361.5	6.0	367.5	2.5	22.3		1.46	1.3	0.5	25.1
6-24E	202.5	7.0	209.5	0.0	22.5	2.28	2.62	2.6	0.0	27.7
6-24E	194.5	1.0	195.5	0.0	22.5		1.94	0.4	0.0	24.8
6-25E	214.5	2.0	216.5	3.0	24.0	2.43	.35	0.7	1.1	25.1
6-25E	192.5	0.0	192.5	0.0	24.0		.65	0.0	0.0	24.7
6-29N	249.5	2.0	251.5	0.0	23.8	2.73	.05	0.6	0.0	24.5
6-29N	515.5	10.0	525.5	5.0	23.8		.67	1.5	0.7	26.0
6-29E	356.5	0.0	356.5	0.5	23.8	2.41	.86	0.0	0.1	24.7
6-29E	381.5	26.0	407.5	1.5	23.8		.14	4.9	0.3	28.3
	6510.5	149.0	6659.5	53.0	22.7% (s=1.51) (n=12)		0.91% (s=1.29) (n=22)	1.7% (s=1.31) (n=22)	.62% (s=0.52) (n=22)	25.3% (s=1.697) (n=22)

RESULTS: Point Counts, Multiple Determinations, Outcrop #1, Bedding Unit #1

Slide	Grain	Over-growth	Total	Pressure Solution	% Porosity Image Analysis		% Adularia	% Quartz Cement	% Pressure Solution	% Porosity Minus Cement
					$\bar{x}$ %	S				
1-10Na	537.0	22.5	559.5	2.0	14.6	2.07	0.0	3.4	0.3	18.0
1-10Na	217.5	21.0	238.5	1.0	14.6	2.07		7.5	0.4	22.1
1-10Na	123.5	11.5	135.0	0.0	14.6	2.07		7.2	0.0	21.8
1-10Na	67.5	4.0	71.5	0.0	14.6	2.07		4.8	0.0	19.4
1-10Na	203.5	7.0	210.5	2.5	14.6	2.07		2.8	1.0	17.4
1-10Na	184.5	13.0	197.5	0.0	14.6	2.07		5.6	0.0	20.2
1-10Na	140.5	8.5	149.0	0.0	14.6	2.07		4.9	0.0	19.5
1-10Na	212.5	18.5	231.0	1.0	14.6	2.07		6.8	0.4	21.4
1-10Na	82.0	11.0	93.0	0.0	14.6	2.07		10.1	0.0	24.7
1-10Na	194.0	8.5	202.5	1.0	14.6	2.07		3.6	0.4	18.2
1-10Na	134.0	17.0	151.5	0.0	14.6	2.07		9.6	0.0	24.2
1-10Na	178.0	4.5	182.5	2.0	14.6	2.07		2.1	0.9	16.7
1-10Na	284.0	12.5	296.5	1.0	14.6	2.07		3.6	0.3	18.2
1-10Na	538.5	29.5	568.0	11.5	14.6	2.07		4.4	1.7	19.0
1-10Na	228.0	16.0	244.0	2.0	14.6	2.07		5.6	0.7	20.2
1-10Na	99.0	9.0	108.0	1.0	14.6	2.07		7.1	0.8	21.7
1-10Na	707.0	39.5	746.5	7.0	14.6	2.07		4.5	0.8	19.1
1-10Na	337.0	17.0	354.0	8.5	14.6	2.07		4.1	2.1	18.7
1-10Na	124.0	17.0	141.0	0.0	14.6	2.07		10.3	0.0	24.9
1-10Na	117.5	4.0	121.5	0.0	14.6	2.07		2.8	0.0	17.4
	4710.0	291.5	5001.5	40.5	14.6% (s=2.07) (n=36)		0.0%	5.0% (s=2.46) (n=20)	0.69% (s=0.60) (n=20)	19.6% (s=2.46) (n=20)

RESULTS: Point Counts, Multiple Determinations, Outcrop 3, Bedding Unit 1

Slide	Total	Pressure Solution	% Porosity Image Analysis		% Adularia	% Quartz Cement	% Pressure Solution	% Porosity Minus Cement
			$\bar{\%}$	$\bar{S}$				
2-5N	1076	14.5	24.1	2.61	0.0	0.0	1.3	24.1
2-5N	1076	12.0	24.1	2.61			1.1	
2-5N	1076	8.0	24.1	2.61			0.7	
2-5N	1076	7.5	24.1	2.61			0.7	
2-5N	1076	8.5	24.1	2.61			0.8	
2-5N	1855	19.5	24.1	2.61			1.1	
2-5N	1855	13.0	24.1	2.61			0.7	
2-5N	1855	29.5	24.1	2.61			1.6	
2-5N	1855	18.5	24.1	2.61			1.0	
2-5N	1855	39.5	24.1	2.61			2.1	
2-5N	1855	30.0	24.1	2.61			1.6	
2-5N	1855	23.5	24.1	2.61			1.3	
2-5N	1855	19.5	24.1	2.61			1.1	
2-5N	1855	19.5	24.1	2.61			1.1	
2-5N	1855	11.5	24.1	2.61			0.6	
2-5N	1855	9.5	24.1	2.61			0.5	
2-5N	1855	18.0	24.1	2.61			1.0	
2-5N	1855	12.5	24.1	2.61			0.7	
2-5N	1855	13.0	24.1	2.61			0.7	
2-5N	1855	14.5	24.1	2.61			0.8	
2-5N	1855	11.0	24.1	2.61			0.6	
2-5N	1940	19.0	24.1	2.61			1.0	
2-5N	1076	8.0	24.1	2.61			0.7	
	38076	380.0	24.1% (s=2.61) (s=36)		0.0%	0.0%	1.0% (s=.39) (s=23)	24.1% (s=2.61) (n=36)

RESULTS: Point Counts, Multiple Determinations, Outcrop #2, Bedding #1a

Slide	Grain	Over-growth	Total	Pressure Solution	% Porosity Image Analysis $\bar{x}$	% Porosity Image Analysis S	% Adularia	% Quartz Cement	% Pressure Solution	% Porosity Minus Cement
3-25E	370.5	35.5	406.0	2.0	19.2	2.91	0.0	7.1	0.4	26.3
3-25E	501.0	24.5	525.5	7.0	19.2	2.91	.42	3.8	1.1	23.4
3-25E	271.0	25.5	296.5	1.0	19.2	2.91	0.0	6.9	0.3	26.1
3-25E	121.5	10.0	131.5	1.0	19.2	2.91	0.0	6.1	0.6	25.3
3-25E	227.5	14.0	241.5	1.5	19.2	2.91	.47	4.7	0.5	24.4
3-25E	343.0	2.0	345.0	0.0	19.2	2.91	.29	0.5	0.0	20.0
3-25E	340.0	14.5	354.5	6.5	19.2	2.91	0.0	3.3	1.5	22.5
3-25E	196.0	23.0	219.0	0.0	19.2	2.91	0.0	8.5	0.0	27.7
3-25E	281.0	21.5	302.5	0.5	19.2	2.91	.67	5.7	0.1	25.6
3-25E	339.0	14.5	353.5	3.5	19.2	2.91	.18	3.3	0.8	22.7
3-25E	493.5	17.0	510.5	11.0	19.2	2.91	.80	2.7	1.7	22.7
3-25E	727.5	30.5	758.0	2.5	19.2	2.91	.52	3.3	0.3	23.0
3-25E	471.5	14.5	486.0	6.5	19.2	2.91	.05	2.4	1.1	21.7
3-25E	239.5	2.0	241.5	0.5	19.2	2.91	.36	0.7	0.2	20.3
3-25E	205.0	9.0	214.0	0.0	19.2	2.91	.15	3.4	0.0	22.8
3-25E	872.5	33.0	905.5	9.0	19.2	2.91	0.0	2.9	0.8	22.1
3-25E	229.0	7.5	236.5	2.0	19.2	2.91	.52	2.6	0.7	22.3
3-25E	340.5	9.0	349.5	1.0	19.2	2.91	.26	2.1	0.2	21.6
3-25E	241.0	5.5	246.5	1.5	19.2	2.91	0.0	1.8	0.5	21.0
3-25E	218.0	9.5	227.5	1.5	19.2	2.91	0.0	3.4	0.5	22.6
	7028.5	322.5	7351.0	58.5	19.2% (s=2.91) (n=36)		0.25% (s=0.26) (n=20)	3.5% (s=2.13) (n=20)	0.64% (s=0.49) (n=20)	23.0% (s=2.08) (n=20)

RESULTS: Point Counts, Multiple Determinations, Outcrop 3, Bedding Unit 2

Slide	Total	Pressure Solution	% Porosity Image Analysis		% Adularia	% Quartz Cement	% Pressure Solution	% Porosity Minus Cement
			%	S				
4-2N	1855	14.5	24.0	3.07	0.0	0.0	0.7	24.0
4-2N	1855	20.0	24.0	3.07			0.9	
4-2N	1855	19.5	24.0	3.07			0.9	
4-2N	1855	11.5	24.0	3.07			0.5	
4-2N	1855	29.5	24.0	3.07			1.4	
4-2N	1855	13.5	24.0	3.07			0.6	
4-2N	1855	16.0	24.0	3.07			0.7	
4-2N	1855	20.5	24.0	3.07			1.0	
4-2N	1855	8.5	24.0	3.07			0.4	
4-2N	1855	8.0	24.0	3.07			0.4	
4-2N	1855	14.0	24.0	3.07			0.6	
4-2N	1855	18.5	24.0	3.07			0.9	
4-2N	1855	12.0	24.0	3.07			0.6	
4-2N	1855	8.0	24.0	3.07			0.4	
4-2N	1855	10.5	24.0	3.07			0.5	
4-2N	1855	7.0	24.0	3.07			0.3	
4-2N	1855	12.0	24.0	3.07			0.6	
4-2N	1855	20.0	24.0	3.07			0.9	
4-2N	1855	12.0	24.0	3.07			0.6	
4-2N	1855	12.0	24.0	3.07			0.6	
	37100	287.5	24.0% (s=3.07) (n=20)		0.0%	0.0%	0.77% (s=0.26) (n=20)	24.0% (s=3.07) (n=20)

RESULTS: Point Counts, Multiple Determinations, Outcrop #2, Bedding Unit #1b

Slide	Grain	Over-growth	Total	Pressure Solution	% Porosity Image Analysis		% Adularia	% Quartz Cement	% Pressure Solution	% Porosity Minus Cement
					$\bar{x}$ %	S				
5-19E	160.5	4.0	164.5	2.0	20.6	2.83	.80	1.9	1.0	23.3
5-19E	567.5	26.5	594.0	8.0	20.6	2.83	.46	3.5	1.1	24.6
5-19E	175.5	14.0	189.5	2.0	20.6	2.83	.21	5.9	0.8	26.7
5-19E	284.5	20.5	305.0	5.0	20.6	2.83	.22	5.3	1.3	26.1
5-19E	635.5	27.0	662.5	4.5	20.6	2.83	.03	3.2	0.5	23.8
5-19E	468.0	26.5	494.5	1.0	20.6	2.83	.46	4.3	0.2	25.4
5-19E	203.5	13.5	217.0	0.0	20.6	2.83	.16	4.9	0.0	25.7
5-19E	216.0	6.0	222.0	1.0	20.6	2.83	.05	2.1	0.4	22.8
5-19E	394.0	8.5	402.5	2.0	20.6	2.83	0.0	1.7	0.4	22.3
5-19E	364.5	20.0	384.5	1.5	20.6	2.83	.19	4.1	0.3	24.9
5-19E	109.5	8.0	117.5	1.5	20.6	2.83	.11	5.4	1.0	26.1
5-19E	166.5	17.0	183.5	0.0	20.6	2.83	.38	7.4	0.0	28.4
5-19E	98.5	2.5	101.0	0.0	20.6	2.83	.05	2.0	0.0	22.7
5-19E	228.0	12.0	240.0	1.0	20.6	2.83	.24	4.0	0.3	24.8
5-19E	440.0	30.0	470.0	3.5	20.6	2.83	0.0	5.1	0.6	25.7
5-19E	237.5	17.5	255.0	5.0	20.6	2.83	.38	5.4	1.6	26.4
5-19E	55.5	7.5	62.5	0.0	20.6	2.83	.27	9.5	0.0	30.4
5-19E	421.0	28.0	449.0	8.0	20.6	2.83	.32	5.0	1.4	25.9
5-19E	198.5	14.5	213.0	0.0	20.6	2.83	.22	5.4	0.0	26.2
5-19E	224.5	8.0	232.5	1.5	20.6	2.83	.32	2.7	0.5	23.7
	5648.5	311.5	5960.0	47.5	20.6% (s=2.83) (n=20)		0.24% (s=0.19) (n=20)	4.1% (s=1.95) (n=20)	0.63% (s=0.51) (n=20)	24.9% (s=1.91) (n=20)

RESULTS: Point Counts, Multiple Determinations, Outcrop #2, Bedding Unit #2

Slide	Grain	Over-growth	Total	Pressure Solution	% Porosity Image Analysis		% Adularia	% Quartz Cement	% Pressure Solution	% Porosity Minus Cement
					$\bar{\%}$	$\bar{S}$				
6-25N	524.0	1.5	525.5	7.0	25.1	1.84	1.22	0.2	1.0	26.5
6-25N	363.5	10.0	373.5	4.0	25.1	1.84	.48	2.0	0.8	27.6
6-25N	270.0	6.0	276.0	0.5	25.1	1.84	.85	1.6	0.1	27.6
6-25N	386.0	8.5	294.5	0.5	25.1	1.84	.61	1.6	0.1	27.3
6-25N	290.0	1.0	291.0	4.0	25.1	1.84	0.0	0.3	1.0	25.4
6-25N	301.5	4.0	305.5	4.5	25.1	1.84	.37	1.0	1.1	26.5
6-25N	339.0	1.5	340.0	2.5	25.1	1.84	.53	0.3	0.6	25.9
6-25N	536.0	4.0	540.5	6.5	25.1	1.84	0.0	0.6	0.9	25.7
6-25N	247.5	3.0	250.5	2.5	25.1	1.84	.50	0.9	0.7	26.5
6-25N	284.0	2.5	286.5	2.5	25.1	1.84	.61	0.7	0.7	26.4
6-25N	351.0	13.0	364.0	0.0	25.1	1.84	.77	2.7	0.0	28.6
6-25N	202.0	0.0	202.0	3.0	25.1	1.84	1.06	0.0	1.1	26.2
6-25N	176.0	3.0	179.0	3.0	25.1	1.84	1.65	1.3	1.3	28.1
6-25N	478.5	6.0	484.5	3.0	25.1	1.84	1.51	0.9	0.5	27.5
6-25N	416.0	2.5	418.5	1.5	25.1	1.84	2.00	0.4	0.3	27.5
6-25N	344.0	4.0	348.0	11.0	25.1	1.84	.11	0.9	2.4	26.1
6-25N	404.0	4.0	408.0	2.5	25.1	1.84	.32	0.7	0.5	26.2
6-25N	176.0	7.5	183.5	2.5	25.1	1.84	.46	3.1	1.0	28.7
6-25N	306.0	4.5	310.5	3.0	25.1	1.84	1.02	1.1	0.7	27.2
6-25N	276.0	3.0	279.0	2.5	25.1	1.84	.70	0.8	0.7	26.6
6-25N	175.0	4.0	179.0	0.5	25.1	1.84	.40	1.7	0.2	27.2
6-25N	6846.0	93.5	6939.5	67.0	25.1% (s=1.84) (n=21)		0.72% (s=0.53) (n=21)	1.0% (s=0.80) (n=21)	0.72% (s=0.53) (n=21)	26.8% (s=0.91) (n=21)